

# Influence of the spin-dependent quasiparticle distribution on the Josephson current through a ferromagnetic weak link

A. M. Bobkov and I. V. Bobkova

*Institute of Solid State Physics, Chernogolovka, Moscow reg., 142432 Russia*

(Dated: March 29, 2019)

The Josephson current flowing through ferromagnetic weak links is studied theoretically under the condition that the quasiparticle distribution over energy states in the interlayer is spin-dependent. In particular, two types of ferromagnetic weak links are considered. The first one is S/N/F/N/S junction, where the interlayer is composed of two normal metal regions with a spiral ferromagnet layer sandwiched between them. The second system is S/N/S junction with magnetic S/N interfaces. It is shown that the interplay between the spin-dependent quasiparticle distribution, which is generated in the interlayer, and the triplet superconducting correlations induced by the proximity effect between the superconducting leads and ferromagnetic elements of the interlayer, leads to the appearance of an additional contribution to the Josephson current. This additional contribution  $j_t$  can be extracted from the full Josephson current in experiment. Moreover, we propose the experimental setup, where the contributions given by the short-range (SRTC) and long-range (LRTC) components of triplet superconducting correlations in the interlayer can be measured separately. For the case of tunnel junctions these measurements can provide direct information about the anomalous Green's function components describing SRTC and LRTC. In addition, it is shown that for S/N/S junction with magnetic interfaces the appearance of  $j_t$  can considerably enhance the critical Josephson current with respect to the case of equilibrium nonmagnetic S/N/S junction with the same S/N interface conductances. For S/N/S junction it is also found that under the considered conditions the dependence of the Josephson current on temperature can be nontrivial: at first the current rises upon temperature increasing and only after that starts to decline.

PACS numbers: 74.45.+c, 74.50.+r

## I. INTRODUCTION

Interplay between superconductivity and ferromagnetism in layered mesoscopic structures offers an arena of interesting physics to explore. By now it is already well known that so-called odd-frequency triplet pairing correlations are generated in hybrid superconductor/ferromagnet (S/F) structures<sup>1,2</sup>. The essence of this pairing state is the following. The wave function of a Cooper pair  $\langle \psi_{\sigma_1}(\mathbf{r}_1, t_1) \psi_{\sigma_2}(\mathbf{r}_2, t_2) \rangle$  must be an odd function with respect to permutations of the two electrons. Consequently, in the momentum representation the wave function of a *triplet* Cooper pair has to be an odd function of the orbital momentum for equal times  $t_1 = t_2$ , that is, the orbital angular momentum  $L$  is an odd number. Thus, the triplet superconducting condensate is sensitive to the presence of impurities, because only the s-wave ( $L = 0$ ) singlet condensate is not sensitive to the scattering by nonmagnetic impurities (Anderson theorem). S/F hybrid structures are usually composed of rather impure materials. Therefore, according to the Pauli principle equal time triplet correlations should be suppressed there. However, another possibility for the triplet pairing exists. In the Matsubara representation the wave function of a triplet pair can be an odd function of the Matsubara frequency and an even function of the momentum. Then the sum over all frequencies is zero and therefore the Pauli principle for the equal-time wave function is not violated. These are the odd-frequency triplet pairing correlations, which are realized in S/F structures.

If there is no a source of spin-flip processes in the considered structure (that is the magnetizations of all the magnetic elements, which are present in the system, are aligned with the only one axis) then the Cooper pairs penetrating into the nonsuperconducting part of the structure consist of electrons with opposite spins. Their wave function is the sum of a singlet component and a triplet component with zero total spin projection  $S_z = 0$  on the quantization axis. The resulting state has common origin with the famous LOFF-state<sup>3,4</sup> and can be referred to as its mesoscopic analogue. This mesoscopic LOFF-state was predicted theoretically<sup>5,6</sup> and observed experimentally<sup>7-11</sup>. In this state Cooper pair acquires the total momentum  $2Q$  or  $-2Q$  inside the ferromagnet as a response to the energy difference between the two spin directions. Here  $Q \propto h/v_F$ , where  $h$  is an exchange energy and  $v_F$  is the Fermi velocity. Combination of the two possibilities results in the spatial oscillations of the condensate wave function  $\Psi(x)$  in the ferromagnet along the direction normal to the SF interface<sup>12</sup>.  $\Psi_s(x) \propto \cos(2Qx)$  for the singlet Cooper pair and  $\Psi_t(x) \propto \sin(2Qx)$  for the triplet Cooper pair. The same picture is also valid in the diffusive limit. However, there is an extra decay of the condensate wave function due to scattering in this case. In the regime  $h \gg |\Delta|$ , where  $\Delta$  is a superconducting order parameter in the leads, the decay length is equal to the magnetic coherence length  $\xi_F = \sqrt{D/h}$ , while the oscillation period is given by  $2\pi\xi_F$ . Here  $D$  is the diffusion constant in the ferromagnet,  $\hbar = 1$  throughout the paper. Due to the fact that the decay length  $\xi_F$  is rather short (much less than the superconducting

coherence length  $\xi_S = \sqrt{D/\Delta}$  the sum of  $\Psi_s(x)$  and  $\Psi_t(x)$  (corresponding to  $S_z = 0$ ) can be considered as a short-range component (SRC) of the pairing correlations induced by the proximity effect in the ferromagnet.

The situation changes if the magnetization orientation is not fixed. The examples are domain walls, spiral ferromagnets, spin-active interfaces, etc. In such a system not only the singlet and triplet  $S_z = 0$  components exist, but also the odd-frequency triplet component with  $S_z = \pm 1$  arises in the nonsuperconducting region. The latter component penetrates the ferromagnet over a large distance, which does not depend on the exchange field and is of the order of  $\xi_N = \sqrt{D/T}$ . So, this triplet component can be considered as the long-range triplet component (LRTC). Various superconducting hybrid structures, where LRTC can arise, were considered in the literature (See Refs. 2, 13, 14 and references therein). In addition, the creation of LRTC was theoretically predicted in structures containing domain walls<sup>15,16</sup>, spin-active interfaces<sup>17,18</sup>, spiral ferromagnets<sup>19–21</sup> and multilayered SFS systems<sup>22,23</sup>. There are several experimental works, where the long-range Josephson effect<sup>24–26</sup> and the conductance of a spiral ferromagnet attached to two superconductors<sup>27</sup> were measured. These results give quite convincing evidence of LRTC existence.

Practically all the discussed above papers are devoted to investigation of an odd-frequency triplet component under the condition that the energy distribution of quasiparticles is equilibrium and spin-independent. However, as it was shown recently<sup>28</sup>, the creation of spin-dependent quasiparticle distribution in the interlayer of SFS junction leads to appearance of the additional contribution to the Josephson current through the junction. This additional supercurrent flows via vector part  $\mathbf{N}_{j,t}$  of supercurrent-carrying density of states, which does not contribute to the Josephson current in a junction with  $s$ -wave superconductor leads if the quasiparticle distribution in the interlayer is spin-independent. Below we briefly describe how this effect arises.

The energy spectrum of the superconducting correlations is expressed in a so-called supercurrent-carrying density of states (SCDOS)<sup>29–32</sup>. This quantity represents the density of states weighted by a factor proportional to the current that each state carries in a certain direction. Under equilibrium conditions the supercurrent can be expressed via the SCDOS as<sup>31</sup>

$$j \propto \int d\varepsilon N_j(\varepsilon) \tanh \varepsilon/2T, \quad (1)$$

where  $\varepsilon$  stands for the quasiparticle energy,  $\tanh \varepsilon/2T = \varphi(\varepsilon)$  is the equilibrium distribution function and  $N_j(\varepsilon)$  is SCDOS. In the presence of spin effects SCDOS becomes a matrix  $2 \times 2$  in spin space and can be represented as  $\hat{N}_j = N_{j,s} + \mathbf{N}_{j,t}\boldsymbol{\sigma}$ , where  $\sigma_i$  are Pauli matrices in spin space. Scalar in spin space part of SCDOS  $N_{j,s}$  is referred to as the singlet part of SCDOS in the paper and vector part  $\mathbf{N}_{j,t}$  is referred to as the triplet part.  $\mathbf{N}_{j,t}$  is directly proportional to the triplet part of the condensate wave

function. It is well known that the spin supercurrent cannot flow through the singlet superconducting leads. Therefore,  $\mathbf{N}_{j,t}$  does not contribute to the supercurrent in equilibrium. Having in mind that the triplet part of SCDOS is even function of quasiparticle energy, one can directly see that this is indeed the case. Otherwise, if the distribution function becomes spin-dependent, that is  $\hat{\varphi}(\varepsilon) = \varphi_0(\varepsilon) + \boldsymbol{\varphi}(\varepsilon)\boldsymbol{\sigma}$ , the supercurrent carried by the SCDOS triplet component  $\mathbf{N}_{j,t}$  in the ferromagnet is non-zero because the scalar product  $\mathbf{N}_{j,t}(\varepsilon)\boldsymbol{\varphi}(\varepsilon)$  contributes to the spinless supercurrent in this case<sup>28</sup>.

As it is obvious from what discussed above, the spin independent nonequilibrium quasiparticle distribution does not result in an additional contribution to the supercurrent flowing via  $\mathbf{N}_{j,t}$ . However, it is worth noting here that the effect of the spin independent nonequilibrium distribution function has been considered as well<sup>33</sup>. It was shown that in the limit of small exchange fields  $h \ll |\Delta|$  the combined effect of the exchange field and the nonequilibrium distribution function is also nontrivial. For instance, part of the field-suppressed supercurrent can be recovered by adjusting a voltage between additional electrodes, which controls the distribution function.

In the present paper we continue investigation of the interplay between the triplet correlations and spin-dependent quasiparticle distribution. We consider Josephson junctions of dirty  $s$ -wave superconductors with complicated interlayers. One of them is S/N/S junction, where the S/N interfaces are magnetic and the other is multilayered S/N/F/N/S junction, where a layer made of a weak ferromagnetic alloy having exchange field  $\Delta \ll h \ll \varepsilon_F$  is sandwiched between two normal metal layers. The direction of the F layer magnetization is assumed to be nonuniform in order to have a possibility of LRTC investigation. The simultaneous presence of the triplet correlations and spin-dependent quasiparticle distribution in the interlayer again results in appearance of the additional contribution to the supercurrent flowing via  $\mathbf{N}_{j,t}$ . It is shown that the existence of such a contribution (i) offers an opportunity to obtain an easily controllable Josephson current manifesting a number of  $0-\pi$  transitions as a function of a voltage applied to the additional electrodes attached to the interlayer region and (ii) even more interesting from the fundamental point of view that by measuring the supercurrent as a function of this voltage one can obtain a detailed information about the structure of triplet correlations induced in the interlayer. While all the experiments described above give unambiguous signatures of the fact that the odd-frequency triplet correlations do exist in hybrid SF systems, they do not allow for direct investigation of the triplet anomalous Green function in dependence on energy. For example, Josephson current in equilibrium is only carried by the scalar part of SCDOS  $N_{j,s}$ . Surely, it is modified by the presence of the triplet component (and, in particular, manifests weakly decaying behavior if LRTC is present in the system). However,  $N_{j,s}$  is not directly proportional

to the triplet anomalous Green function, but can contain it only in a nonlinear way. The other measurable quantity in equilibrium is the local density of states (LDOS), where the odd-frequency triplet component manifests itself as a zero-energy peak. This effect has been studied as for SF bilayers so as for SN bilayers with magnetic interfaces<sup>34–39</sup>. However, LDOS is also not directly proportional to the triplet anomalous Green's function. The oscillating behavior of the critical temperature as a function of an SF bilayer width (See, for example, Ref. 11 and references therein) is also an excellent fingerprint of the triplet correlations (one-dimensional LOFF state) presence. However, the order parameter in the singlet superconductor S is related only to the singlet part of the anomalous Green function, which is modified by the presence of triplet correlations, but does not allow for their direct observation. On the other hand, in case if the quasiparticle distribution is spin-dependent, quantities, which are directly proportional to the triplet anomalous Green function start to contribute to experimentally observable things. Josephson current under the condition of spin-dependent quasiparticle distribution in the interlayer is one of them.

The paper is organized as follows. In Sec. II the considered model systems are described and the theoretical framework to be used for obtaining our results is established. In Sec. III we present the results of the Josephson current calculation for a multilayered S/NFN/S system under spin-dependent quasiparticle distribution and demonstrate how to obtain from these data an information about the structure of the odd-frequency triplet correlations. Sec. IV is devoted to consideration of SNS junction with magnetic SN interfaces under similar conditions for the quasiparticle distribution in the interlayer. We summarize our finding in Sec. V.

## II. MODEL AND GENERAL SCHEME OF CALCULATIONS

The first system we consider is a multilayer S/NFN/S Josephson junction shown schematically in Fig. 1. It consists of two *s*-wave superconductors (S) and an interlayer composed of two normal layers  $N^l$  and  $N^r$  with a ferromagnetic layer F, sandwiched between them. The *x*-axis is directed along the normal to the junction and the *y*- and *z*-axes are in the junction plane. The coordinates of FN interfaces are  $x = \mp d_F/2$ , while SN interfaces are located at  $x = \mp(d_F + d_N)/2$ . That is, the full length of the F layer is  $d_F$ , while the length of each N layer is  $d_N/2$ . The middle F layer is supposed to be made of a weak ferromagnetic alloy with the exchange field  $h$  satisfying the condition  $\Delta \ll h \ll \varepsilon_F$ . The exchange field of F layer is assumed to be non-homogeneous, what allows for the existence as triplet pairs with opposite spins (SRTC) so as triplet pairs with parallel spins (LRTC) in the interlayer. For simplicity we suppose that  $\mathbf{h} = h(0, \sin \Theta(x), \cos \Theta(x))$ , that

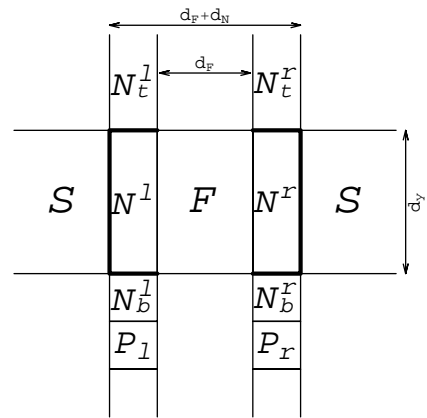


FIG. 1. S/N/F/N/S junction under consideration with the additional electrodes, which are proposed to be used for creation of a spin-dependent quasiparticle distribution in the interlayer.

is the magnetization vector rotates in the F layer (within the junction plane). The rotation angle has a simple *x*-dependence

$$\Theta(x) = \Theta'x, \quad -d_F/2 < x < d_F/2, \quad (2)$$

where  $\Theta'$  does not depend on coordinates. The additional electrodes are supposed to be attached to the N layers in order to make it possible to create a spin-dependent quasiparticle distribution in the interlayer.

We use the formalism of quasiclassical Green-Keldysh functions<sup>40</sup> and assume that the superconductors and all the internal layers are in the diffusive regime. The fundamental quantity for diffusive transport is the momentum average of the quasiclassical Green's function  $\check{g}(\mathbf{r}, \varepsilon, t) = \langle \check{g}(\mathbf{p}_f, \mathbf{r}, \varepsilon, t) \rangle_{\mathbf{p}_f}$ . It is a  $8 \times 8$  matrix form in the product space of Keldysh, particle-hole and spin variables. In the absence of an explicit dependence on time variable the Green's function  $\check{g}(\mathbf{r}, \varepsilon)$  in the interlayer obeys the Usadel equation

$$\frac{D}{\pi} \nabla (\check{g} \nabla \check{g}) + [\varepsilon \tau_3 \sigma_0 \rho_0 - \check{h}, \check{g}] = 0, \quad (3)$$

where  $\tau_i$ ,  $\sigma_i$  and  $\rho_i$  are Pauli matrices in particle-hole, spin and Keldysh spaces, respectively.  $\tau_0$ ,  $\sigma_0$  and  $\rho_0$  stand for the corresponding identity matrices. For simplicity, the diffusion constant  $D$  is supposed to be identical in all three internal layers. The matrix structure of the exchange field is as follows

$$\check{h} = \mathbf{h} \sigma \rho_0 (1 + \tau_3)/2 + \mathbf{h} \sigma^* \rho_0 (1 - \tau_3)/2. \quad (4)$$

The exchange field  $\mathbf{h}$  rotates in the F layer according to the described above model. In the N layers  $\mathbf{h} = 0$ .

The Usadel equation (3) should be supplied with the normalization condition  $\check{g}^2 = \tau_0 \sigma_0 \rho_0$  and is subject to Kupriyanov-Lukichev boundary conditions<sup>41</sup> at S/N and N/F interfaces. It is worth to note that we can safely apply these boundary conditions to the problem of plane

diffusive junction even for high enough dimensionless conductance  $g$  of the SF interface. This can be done in spite of the fact that they are the linear in transparency approximation of more general Nazarov boundary conditions<sup>42</sup>. The reason is that the effective number of interface channels  $N \sim d_y/l$  is large and a separate channel transparency  $T \sim g(l/d_y)$  is usually considerably less than unity. Here  $d_y$  is the junction width in the  $y$ -direction and  $l$  is the mean free path. The barrier conductances of the left and right S/N interfaces are assumed to be identical for simplicity and are denoted as  $G_T$ . Then the boundary conditions at S/N interfaces take the form

$$\check{g}_N \partial_x \check{g}_N = -\alpha \frac{G_T}{2\sigma_N} [\check{g}_N, \check{g}_S] . \quad (5)$$

Here  $\check{g}_N$  is the solution of the Usadel equation (3) at the left ( $x = -(d_N + d_F)/2$ ) or right ( $x = (d_N + d_F)/2$ ) S/N interface.  $\alpha = +1(-1)$  at the left (right) interface.  $\sigma_N$  is the conductivity of N layers and  $\sigma_F$  is the conductivity of F layer (defined for later use).  $\check{g}_S$  stands for the Green's functions at the superconducting leads. Due to the fact that we are mostly interested in the case of low-transparent S/N interfaces below, we can safely neglect the suppression of the superconducting order parameter in the S leads near the interface and take the Green's functions at the superconducting side of the boundaries to be equilibrium and equal to their bulk values. In this case

$$\check{g}_S^K = (\check{g}_S^R - \check{g}_S^A) \tanh \frac{\varepsilon}{2T} , \quad (6)$$

$$\check{g}_S^{R,A} = -i\pi\kappa \cosh \Theta_S^{R,A} \tau_3 \sigma_0 + i\pi\kappa \sinh \Theta_S^{R,A} i\sigma_2 \times \left[ e^{-\frac{i\alpha\chi}{2} \frac{\tau_1 + i\tau_2}{2}} + e^{\frac{i\alpha\chi}{2} \frac{\tau_1 - i\tau_2}{2}} \right] , \quad (7)$$

$$\cosh \Theta_S^{R,A} = \frac{-\kappa i\varepsilon}{\sqrt{|\Delta|^2 - (\varepsilon + \kappa i\delta)^2}} , \quad \sinh \Theta_S^{R,A} = \frac{-\kappa i|\Delta|}{\sqrt{|\Delta|^2 - (\varepsilon + \kappa i\delta)^2}} , \quad (8)$$

where  $\kappa = +1(-1)$  for the retarded (advanced) Green's function,  $\chi$  stands for the order parameter phase difference between the superconducting leads and  $\delta$  is a positive infinitesimal.

We assume the NF interfaces to be absolutely transparent. This approximation simplifies the calculations significantly, but does not influence qualitatively our main conclusions. For this case the boundary conditions at  $x = \mp d_F/2$  take the form

$$\check{g}_N = \check{g}_F , \quad \sigma_N \partial_x \check{g}_N = \sigma_F \partial_x \check{g}_F . \quad (9)$$

The second model system, which we consider in order to study the odd-frequency triplet correlations, is an

S/N/S junction with magnetic S/N interfaces. The full length of the normal region is  $d_N$ , the  $x$ -axis is normal to the junction plane and the interfaces are located at  $x = \mp d_N/2$ . As in the previous case, additional electrodes are attached to the interlayer region for creation of a spin-dependent quasiparticle distribution in the interlayer. The Green's function in the N layer obeys Eq. (3) provided that  $\hbar = 0$ . However, the boundary conditions contain additional terms with respect to Eq. (5) because the transmission properties of spin-up and spin-down electrons into a ferromagnetic metal or a ferromagnetic insulator are different, which gives rise to spin-dependent conductivities (spin-filtering) and spin-dependent phase shifts (spin-mixing) at the interface. The generalized boundary conditions for the diffusive limit can be written in the form<sup>43,44</sup>

$$\check{g}_N \partial_x \check{g}_N = -\alpha \frac{G_T}{2\sigma_N} [\check{g}_N, \check{g}_S] - \alpha \frac{G_{MR}}{2\sigma_N} [\check{g}_N, \{\check{m}_\alpha, \check{g}_S\}] + \alpha \frac{G_\phi \pi}{2\sigma_N} [\check{m}_\alpha, \check{g}_N] , \quad (10)$$

where  $\check{g}_N$  is the Green's function value at the normal side of the appropriate S/N interface (at  $x = \mp d_N/2$ ). As above,  $\check{g}_S$  stands for the Green's function in the superconducting lead and is expressed by Eqs. (6)-(8).  $\check{m}_\alpha = \mathbf{m}_\alpha \sigma \rho_0 (1 + \tau_3)/2 + \mathbf{m}_\alpha \sigma^* \rho_0 (1 - \tau_3)/2$ , where  $\mathbf{m}_\alpha$  is the unit vector aligned with the direction of the left ( $\alpha = +1$ ) or right ( $\alpha = -1$ ) SN interface magnetization. {...} means anticommutator. The second term accounts for the different conductances of different spin directions and  $G_{MR} \sim G_{T,\uparrow} - G_{T,\downarrow}$ . The third term  $\sim G_\phi$  gives rise to spin-dependent phase shifts of quasiparticles being reflected at the interface.  $G_\phi$  has been calculated for some particular microscopic models of the interface<sup>39,43</sup> and can be large enough even if the conductance  $G_T \rightarrow 0$ , corresponding to a ferromagnetic insulator.

In what follows we assume that the S/N interfaces are low-transparent for the both considered systems, that is  $\tilde{G}_T \equiv G_T \xi_S / \sigma_N \ll 1$  and  $\tilde{G}_{MR} \equiv G_{MR} \xi_S / \sigma_N \ll 1$ . This approximation simplifies the calculations considerably, but yet allows us to capture the main effects. In order to calculate the Josephson current through the junction in the leading order of the interface transparency  $\tilde{G}_T$  it is enough to obtain the retarded and advanced Green's functions in the leading order of the transparency. If one makes use of the following definitions for the Green's function elements in the particle-hole space (all the matrices denoted by  $\hat{\cdot}$  are  $2 \times 2$  matrices in spin space throughout the paper)

$$\check{g}^{R,A} = \begin{pmatrix} \hat{g}^{R,A} & \hat{f}^{R,A} \\ \hat{f}^{R,A} & \hat{g}^{R,A} \end{pmatrix} , \quad (11)$$

then one can obtain from the Usadel equation (3) and the appropriate boundary conditions Eq. (5) or (10) that the diagonal in particle-hole space elements of  $\check{g}^{R,A}$  are zero-order in  $\tilde{G}_T$  quantities and take the following form

in the interlayer

$$\begin{aligned}\hat{g}^{R,A} &= -i\kappa\pi \\ \hat{\tilde{g}}^{R,A} &= i\kappa\pi\end{aligned}\quad (12)$$

The off-diagonal in particle-hole space elements of the Green's function are of the first order in  $\tilde{G}_T$  and should be obtained from the linearized Usadel equations, which are to be derived from Eq. (3). It is convenient to represent the off-diagonal elements in the following form

$$\begin{aligned}\hat{f}^{R,A} &= f_s^{R,A}i\sigma_2 + \mathbf{f}_t^{R,A}\boldsymbol{\sigma}i\sigma_2 \\ \hat{\tilde{f}}^{R,A} &= -i\sigma_2\tilde{f}_s^{R,A} - i\sigma_2\tilde{\mathbf{f}}_t^{R,A}\boldsymbol{\sigma},\end{aligned}\quad (13)$$

where  $f_s^{R,A}$  and  $\mathbf{f}_t^{R,A}$  denote the singlet and triplet parts of the anomalous Green's function, respectively. For the case we consider (the magnetization vectors of all the ferromagnetic layers and spin-active interfaces, which are present in the system, are in the junction plane) the out-of-plane  $x$ -component of the triplet part is absent and the linearized Usadel equations for the anomalous Green's function  $\{f_s^{R,A}, \mathbf{f}_t^{R,A}\}$  can be written as follows

$$\begin{aligned}2\varepsilon f_s^{R,A} - 2\mathbf{h}\mathbf{f}_t^{R,A} - i\kappa D\partial_x^2 f_s^{R,A} &= 0 \\ 2\varepsilon \mathbf{f}_t^{R,A} - 2\mathbf{h}f_s^{R,A} - i\kappa D\partial_x^2 \mathbf{f}_t^{R,A} &= 0.\end{aligned}\quad (14)$$

According to the general symmetry relation<sup>45</sup>  $\hat{f}^{R,A}(\varepsilon) = \hat{f}^{R,A*}(-\varepsilon)$  the singlet and triplet parts of  $\hat{f}^{R,A}$  can be expressed via the corresponding parts of  $\hat{f}^{R,A}$  as follows

$$\begin{aligned}\tilde{f}_s(\varepsilon) &= -f_s^*(-\varepsilon) \\ \tilde{\mathbf{f}}_t(\varepsilon) &= \mathbf{f}_t^*(-\varepsilon).\end{aligned}\quad (15)$$

The linearized Usadel equations (14) should be supplemented by the appropriate boundary condition, which are to be obtained by linearization of Eq. (5) or (10) and

at the S/N interfaces take the form

$$\begin{aligned}\partial_x f_{N,s}^{R,A} &= -\alpha \frac{G_T}{\sigma_N} i\kappa\pi \sinh \Theta_S^{R,A} e^{-i\alpha\chi/2} + \alpha \frac{G_\phi}{\sigma_N} i\kappa\mathbf{m}_\alpha \mathbf{f}_{N,t}^{R,A} \\ \partial_x \mathbf{f}_{N,t}^{R,A} &= \alpha \frac{G_\phi}{\sigma_N} i\kappa\mathbf{m}_\alpha f_{N,s}^{R,A},\end{aligned}\quad (16)$$

where  $f_{N,s}^{R,A}$  and  $\mathbf{f}_{N,t}^{R,A}$  are the singlet and triplet part values of the anomalous Green's function at the normal side of the S/N interface.  $G_\phi \neq 0$  only if the S/N interface is spin-active. It is worth to note here that in this linear in  $\tilde{G}_T$  and  $\tilde{G}_{MR}$  approximation the term proportional to  $G_{MR}$  does not enter the boundary conditions.

Boundary conditions at the fully-transparent N/F interfaces are obtained by linearizing Eq. (9) and read as follows

$$\begin{aligned}\hat{f}_N^{R,A} &= \hat{f}_F^{R,A}, \\ \sigma_N \partial_x \hat{f}_N^{R,A} &= \sigma_F \partial_x \hat{f}_F^{R,A}.\end{aligned}\quad (17)$$

Eqs. (14), (16) and (17) allow for the calculation of the retarded and advanced Green's functions in the leading in transparency approximation. However, it is not enough for obtaining of the electric current through the junction, which should be calculated via Keldysh part of the quasiclassical Green's function. For the plane diffusive junction the corresponding expression for the current density reads as follows

$$j = \frac{-\sigma_N}{e} \int_{-\infty}^{+\infty} \frac{d\varepsilon}{8\pi^2} \text{Tr}_4 \left[ \frac{\tau_0 + \tau_3}{2} (\check{g}(x, \varepsilon) \partial_x \check{g}(x, \varepsilon))^K \right], \quad (18)$$

where  $e$  is the electron charge. The expression is written for the normal layer, but it is also valid for the ferromagnetic region with the substitution  $\sigma_F$  for  $\sigma_N$ .  $(\check{g}(x, \varepsilon) \partial_x \check{g}(x, \varepsilon))^K$  is  $4 \times 4$  Keldysh part of the corresponding combination of full Green's function. It is convenient to calculate the current at the S/N interfaces. Then the required combination of the Green's functions can be easily found from Keldysh part of boundary conditions (5) or (10). In addition, we express Keldysh part of the full Green's function via the retarded and advanced components and the distribution function:  $\check{g}^K = \check{g}^R \check{\varphi} - \check{\varphi} \check{g}^A$ . Here the argument  $(x, \varepsilon)$  of all the functions is omitted for brevity. The distribution function is diagonal in particle-hole space:  $\check{\varphi} = \hat{\varphi}(\tau_0 + \tau_3)/2 + \sigma_2 \hat{\varphi} \sigma_2 (\tau_0 - \tau_3)/2$ . Then to the leading (second) order in transparency

---


$$\begin{aligned}\text{Tr}_4 \left[ \frac{\tau_0 + \tau_3}{2} (\check{g}(x, \varepsilon) \partial_x \check{g}(x, \varepsilon))^K \right] &= \frac{\alpha G_T i\pi}{\sigma_N} \left[ (\sinh \Theta_S^R + \sinh \Theta_S^A) \tanh \frac{\varepsilon}{2T} \left( f_{N,s}^R e^{i\alpha\chi/2} + \tilde{f}_{N,s}^A e^{-i\alpha\chi/2} \right) - \right. \\ &\quad \left( f_{N,s}^R \tilde{\varphi}_0^{(0)} - \varphi_0^{(0)} f_{N,s}^A \right) \sinh \Theta_S^A e^{i\alpha\chi/2} + \left( \tilde{f}_{N,s}^R \varphi_0^{(0)} - \tilde{\varphi}_0^{(0)} \tilde{f}_{N,s}^A \right) \sinh \Theta_S^R e^{-i\alpha\chi/2} - \\ &\quad \left( \mathbf{f}_{N,t}^R \tilde{\varphi}^{(0)} - \varphi^{(0)} \mathbf{f}_{N,t}^A \right) \sinh \Theta_S^A e^{i\alpha\chi/2} + \left( \tilde{\mathbf{f}}_{N,t}^R \varphi^{(0)} - \tilde{\varphi}^{(0)} \tilde{\mathbf{f}}_{N,t}^A \right) \sinh \Theta_S^R e^{-i\alpha\chi/2} - \\ &\quad \left. 2i\pi (\cosh \Theta_S^R + \cosh \Theta_S^A) \left( \tanh \frac{\varepsilon}{2T} - \varphi_0^{(0)+(1)} \right) \right] + \frac{2\alpha G_{MR} i\pi}{\sigma_N} \left[ 2i\pi (\cosh \Theta_S^R + \cosh \Theta_S^A) \mathbf{m}_\alpha \varphi^{(0)+(1)} \right],\end{aligned}\quad (19)$$

where  $f_{N,s}^{R,A}$  and  $\mathbf{f}_{N,t}^{R,A}$  are taken at the normal side of the appropriate S/N boundary.  $\varphi_0$  and  $\boldsymbol{\varphi}$  represent the scalar and vector parts of the distribution function  $\hat{\varphi} = \varphi_0 + \boldsymbol{\varphi}\boldsymbol{\sigma}$ , which is also taken at the normal side of the appropriate S/N boundary. The superscripts  $\dots^{(0)}$  and  $\dots^{(0)+(1)}$  of the distribution functions mean that the corresponding quantity is calculated up to the zero and the first orders of magnitude in the interface conductance  $\tilde{G}_T$ , respectively.

In order to calculate the current through the junction one should substitute Eq. (19) into Eq. (18). The resulting expression for the current can be further simplified by taking into account the general symmetry relations between the Green's function elements<sup>45</sup> expressed by Eq. (15) and the ones given below

$$\begin{aligned} f_s^A(\varepsilon) &= f_s^R(-\varepsilon) \\ \mathbf{f}_t^A(\varepsilon) &= -\mathbf{f}_t^R(-\varepsilon) \\ \tilde{\varphi}_0(\varepsilon) &= -\varphi_0(-\varepsilon) \\ \tilde{\boldsymbol{\varphi}}(\varepsilon) &= \boldsymbol{\varphi}(-\varepsilon) . \end{aligned} \quad (20)$$

Then the expression for the current density takes the form

$$\begin{aligned} j = \int_{-\infty}^{\infty} \frac{d\varepsilon}{2\pi e} \Big\{ & \alpha G_T \left( \text{Im} \left[ f_{N,s}^R e^{i\alpha\chi/2} \right] \tanh \frac{\varepsilon}{2T} \text{Re} [\sinh \Theta_S^R] + \right. \\ & \text{Re} \left[ f_{N,s}^R e^{i\alpha\chi/2} \right] \tilde{\varphi}_0^{(0)} \text{Im} [\sinh \Theta_S^R] + \\ & \text{Re} \left[ \mathbf{f}_{N,t}^R e^{i\alpha\chi/2} \right] \tilde{\boldsymbol{\varphi}}^{(0)} \text{Im} [\sinh \Theta_S^R] - \\ & \left. \pi \cosh \Theta_S^R [\varphi_0^{(0)+(1)}(\varepsilon) + \varphi_0^{(0)+(1)}(-\varepsilon)]/2 \right) + \\ & \left. \alpha G_{MR} \pi \cosh \Theta_S^R \mathbf{m}_\alpha [\boldsymbol{\varphi}^{(0)+(1)}(\varepsilon) + \boldsymbol{\varphi}^{(0)+(1)}(-\varepsilon)] \right\} . \end{aligned} \quad (21)$$

The additional contribution to the current, which is absent for a spin-independent distribution function, is given by the third term. As it was mentioned in the introduction, this term (connected to the triplet part of SCDOS) is directly proportional to the triplet anomalous Green's function at the interface. The fifth term also results from vector part of the distribution function, but under the considered conditions it does not contribute to the current, as it is shown below. It is worth to note here that, as it is seen from Eq. (21), the singlet part of SCDOS is only expressed via the singlet part of the anomalous Green's function. However, it does not mean that the triplet correlations do not contribute to the current for the case of spin-independent distribution function. They do contribute, as it was demonstrated by a lot of experiments discussed in the introduction. The point is that for the considered case of the tunnel junction  $f_s$  in general contains long-range contributions resulting from the LRTC (if they are present in the system). It is worth to emphasize that all the aforesaid only concerns the calculation of the current at the interface. If one would calculate the current at an arbitrary point of the interlayer, the corresponding expression would contain  $\mathbf{f}_t$  quadratically. Surely, the current by itself does not depend on

$x$ -coordinate, as it is required by the current conservation.

The distribution function  $\hat{\varphi}^{(0)+(1)}$  entering current (21) should be calculated by making use of the kinetic equation, which is obtained from the Keldysh part of Usadel equation (3). As we only need the distribution function up to the first order in the interface conductance, all the terms accounting for the proximity effect (which are of the second order in  $\tilde{G}_T$ ) drop out and the kinetic equation takes especially simple form (we do not take into account inelastic relaxation in the interlayer)

$$\nabla^2 \hat{\varphi} - \frac{i}{D} [\mathbf{h}(x)\boldsymbol{\sigma}, \hat{\varphi}] = 0 , \quad (22)$$

where the exchange field  $\mathbf{h}(x)$  is determined above for the ferromagnetic layer and vanishes for all the normal regions. For the case of multilayered N/F/N interlayer Eq. (22) should be supplemented by the boundary conditions at the N/F interfaces, which are obtained from Keldysh part of Eqs. (9) and to the considered accuracy take the form

$$\begin{aligned} \hat{\varphi}_F &= \hat{\varphi}_N , \\ \sigma_F \partial_x \hat{\varphi}_F &= \sigma_N \partial_x \hat{\varphi}_N . \end{aligned} \quad (23)$$

The kinetic equation should be also supplemented by the boundary conditions at the S/N interfaces and the interfaces with additional electrodes, attached to the normal regions of the interlayer in order to create a spin-dependent quasiparticle distribution. While the boundary conditions at the interfaces with additional electrodes are discussed below for a particular considered system, the boundary conditions at the S/N interfaces are obtained from the Keldysh part of Eqs. (10) or (5) and to the first order in the interface conductance take the form

$$\begin{aligned} \partial_x \hat{\varphi}^{(0)} &= \frac{\alpha i G_\phi}{2\sigma_N} [\mathbf{m}_\alpha \boldsymbol{\sigma}, \hat{\varphi}^{(0)}] , \\ \partial_x \hat{\varphi}^{(1)} &= -\frac{\alpha G_T}{2\sigma_N} (\cosh \Theta_S^R + \cosh \Theta_S^A) \left( \tanh \frac{\varepsilon}{2T} - \hat{\varphi}^{(0)} \right) - \\ & \frac{\alpha G_{MR}}{\sigma_N} \left[ (\cosh \Theta_S^R + \cosh \Theta_S^A) \tanh \frac{\varepsilon}{2T} \mathbf{m}_\alpha \boldsymbol{\sigma} - \right. \\ & \left. \cosh \Theta_S^R \mathbf{m}_\alpha \boldsymbol{\sigma} \hat{\varphi}^{(0)} - \cosh \Theta_S^A \hat{\varphi}^{(0)} \mathbf{m}_\alpha \boldsymbol{\sigma} \right] + \\ & \frac{\alpha i G_\phi}{2\sigma_N} [\mathbf{m}_\alpha \boldsymbol{\sigma}, \hat{\varphi}^{(1)}] . \end{aligned} \quad (24)$$

### III. S/NFN/S JUNCTION

Now we consider the particular systems. This section is devoted to S/NFN/S Josephson junction. The model assumed for the exchange field of the F layer is already described above. The anomalous Green's function to the first order in S/N conductance  $\tilde{G}_T$  is found according to Eqs. (14), (16) and (17). In order to simplify the final expressions we assume that the magnetization of the F layer rotates slowly, that is  $\Theta' \xi_F \ll 1$ , while  $\Theta' \xi_S \sim 1$

or even larger than unity. This assumption seems to be quite reasonable<sup>2</sup>. Therefore, upon calculating the anomalous Green's functions we disregard all the terms proportional to  $\Theta'\sqrt{D/h}$  and higher powers of this parameter, while keeping the terms, where  $\Theta'$  enters in the dimensionless combination  $\Theta'\sqrt{D/|\varepsilon|}$ . To this accuracy, at the left ( $\alpha = +1$ ) and the right ( $\alpha = -1$ ) S/N interfaces the anomalous Green's function singlet part takes the following form

$$f_s^R = \frac{i\pi G_T}{\sigma_N \lambda_N} \tanh \phi_N \sinh \Theta_S^R e^{-i\alpha\chi/2} + \frac{i\pi G_T \sinh \Theta_S^R}{2\sigma_F \cosh^2 \phi_N} \times \left[ \frac{\cos(\chi/2) \cosh \phi_+}{\lambda_+ \sinh \phi_+ + \rho \cosh \phi_+} - \frac{i\alpha \sin(\chi/2) \sinh \phi_+}{\lambda_+ \cosh \phi_+ + \rho \sinh \phi_+} + \frac{\cos(\chi/2) \cosh \phi_-}{\lambda_- \sinh \phi_- + \rho \cosh \phi_-} - \frac{i\alpha \sin(\chi/2) \sinh \phi_-}{\lambda_- \cosh \phi_- + \rho \sinh \phi_-} \right], \quad (25)$$

where  $\lambda_{\pm} = \sqrt{h/D}(1 \mp i)$ ,  $\lambda_N = \sqrt{-2i(\varepsilon + i\delta)/D}$ ,  $\phi_{\pm} = \lambda_{\pm} d_F/2$ ,  $\phi_N = \lambda_N d_N/2$  and  $\rho = (\sigma_N/\sigma_F)\lambda_N \tanh \phi_N$ .

The triplet part of the anomalous Green's function can be represented as

$$\mathbf{f}_t^R = (0, f_y, f_z), \quad f_y = \sin \Theta(x) f_{SR}(x) - \cos \Theta(x) f_{LR}(x), \quad f_z = \cos \Theta(x) f_{SR}(x) + \sin \Theta(x) f_{LR}(x), \quad (26)$$

where the  $z$ -axis is aligned with the direction of the exchange field in the middle of the F layer (at  $x = 0$ ).  $f_{SR}$  ( $f_{LR}$ ) is formed by the Cooper pairs composed of the electrons with opposite (parallel) spins. Consequently,  $f_{SR}$  is rapidly decaying in the interlayer, while  $f_{LR}$  is slowly decaying, as it is seen from what follows. We are interested in the values of the triplet component at the S/N interfaces, where  $\sin \Theta(x) \equiv -\alpha \sin \Theta \equiv -\alpha \sin [\Theta' d_F/2]$  and

$$f_{SR} = -\frac{i\pi G_T \sinh \Theta_S^R}{2\sigma_F \cosh^2 \phi_N} \left[ \frac{\cos(\chi/2) \cosh \phi_+}{\lambda_+ \sinh \phi_+ + \rho \cosh \phi_+} - \frac{i\alpha \sin(\chi/2) \sinh \phi_+}{\lambda_+ \cosh \phi_+ + \rho \sinh \phi_+} - \frac{\cos(\chi/2) \cosh \phi_-}{\lambda_- \sinh \phi_- + \rho \cosh \phi_-} + \frac{i\alpha \sin(\chi/2) \sinh \phi_-}{\lambda_- \cosh \phi_- + \rho \sinh \phi_-} \right], \quad f_{LR} = -\frac{i\pi G_T \sinh \Theta_S^R}{2\sigma_F \cosh^2 \phi_N} \left\{ \frac{\Theta' i \sin(\chi/2) \cosh \phi_t}{\rho \cosh \phi_t + \lambda_t \sinh \phi_t} \left[ \frac{\sinh \phi_+}{\lambda_+ \cosh \phi_+ + \rho \sinh \phi_+} - \frac{\sinh \phi_-}{\lambda_- \cosh \phi_- + \rho \sinh \phi_-} \right] - \frac{\alpha \Theta' \cos(\chi/2) \sinh \phi_t}{\rho \sinh \phi_t + \lambda_t \cosh \phi_t} \left[ \frac{\cosh \phi_+}{\lambda_+ \sinh \phi_+ + \rho \cosh \phi_+} - \frac{\cosh \phi_-}{\lambda_- \sinh \phi_- + \rho \cosh \phi_-} \right] \right\}, \quad (27)$$

where  $\lambda_t = \sqrt{\Theta'^2 - 2i(\varepsilon + i\delta)/D}$  and  $\phi_t = \lambda_t d_F/2$ .

The fact that  $f_{SR}$  rapidly decays in the ferromagnetic region and, consequently, represents the SRTC can be easily seen from Eq. (27) in the limit of thick enough F layer:  $d_F/\xi_F \gg 1$ . Let us consider  $f_{SR}$  at the left S/N interface (the left interface is chosen just for definiteness). It can be rewritten in the form

$$f_{SR} = f_{SR}^l e^{-i\chi/2} + f_{SR}^r e^{i\chi/2}, \quad (28)$$

where  $f_{SR}^l$  is generated by the proximity effect at the left S/N interface itself and  $f_{SR}^r$  comes from the right S/N interface. To the leading order in the parameter  $e^{-d_F/\xi_F}$  one obtains from Eq. (27)

$$f_{SR}^l = -\frac{i\pi G_T \sinh \Theta_S^R}{2\sigma_F \cosh^2 \phi_N} \left[ \frac{1}{\lambda_+ + \rho} - \frac{1}{\lambda_- + \rho} \right], \quad f_{SR}^r = -\frac{i\pi G_T \sinh \Theta_S^R}{\sigma_F \cosh^2 \phi_N} \left[ \frac{\lambda_+ e^{-\lambda_+ d_F}}{(\lambda_+ + \rho)^2} - \frac{\lambda_- e^{-\lambda_- d_F}}{(\lambda_- + \rho)^2} \right]. \quad (29)$$

On the contrary,  $f_{LR}$  does not contain the small factor  $e^{-d_F/\xi_F}$  in the leading approximation and, therefore, describes the LRTC. Again, if  $f_{LR}$  is represented as

$$f_{LR} = f_{LR}^l e^{-i\chi/2} + f_{LR}^r e^{i\chi/2}, \quad (30)$$

the corresponding components take the following form

$$f_{LR}^l = \frac{i\pi G_T \sinh \Theta_S^R}{2\sigma_F \cosh^2 \phi_N} \left[ \frac{1}{\lambda_+ + \rho} - \frac{1}{\lambda_- + \rho} \right] \times \frac{\Theta'(\lambda_t \cosh[2\phi_t] + \rho \sinh[2\phi_t])}{(\rho \cosh \phi_t + \lambda_t \sinh \phi_t)(\rho \sinh \phi_t + \lambda_t \cosh \phi_t)}, \quad f_{LR}^r = -\frac{i\pi G_T \sinh \Theta_S^R}{2\sigma_F \cosh^2 \phi_N} \left[ \frac{1}{\lambda_+ + \rho} - \frac{1}{\lambda_- + \rho} \right] \times \frac{\Theta' \lambda_t}{(\rho \cosh \phi_t + \lambda_t \sinh \phi_t)(\rho \sinh \phi_t + \lambda_t \cosh \phi_t)}. \quad (31)$$

As it is seen from Eq. (31), the characteristic decay length of  $f_{LR}$  in the F layer is  $|\lambda_t|^{-1}$ . It is much larger than  $\xi_F$  for the considered case  $\xi_F \ll \Theta'^{-1}$ .

To the considered accuracy the singlet component of the anomalous Green's function also decays at the distance  $\sim \xi_F$  in the F layer, just as the SRTC  $f_{SR}$  does, because it is also composed of the electron pairs with antiparallel spin directions. Indeed, if  $f_s^R$  at the left boundary is also represented as

$$f_s^R = f_s^l e^{-i\chi/2} + f_s^r e^{i\chi/2}, \quad (32)$$

then in the limit  $d_F/\xi_F \gg 1$  it is obtained from Eq. (25)

that

$$f_s^l = \frac{i\pi G_T}{\sigma_N \lambda_N} \tanh \phi_N \sinh \Theta_S^R + \frac{i\pi G_T \sinh \Theta_S^R}{2\sigma_F \cosh^2 \phi_N} \left[ \frac{1}{\lambda_+ + \rho} + \frac{1}{\lambda_- + \rho} \right],$$

$$f_s^r = \frac{i\pi G_T \sinh \Theta_S^R}{\sigma_F \cosh^2 \phi_N} \left[ \frac{\lambda_+ e^{-\lambda_+ d_F}}{(\lambda_+ + \rho)^2} + \frac{\lambda_- e^{-\lambda_- d_F}}{(\lambda_- + \rho)^2} \right]. \quad (33)$$

Therefore, the main contribution to the Josephson current Eq. (21) is given by the LRTC component  $f_{LR}$  of the anomalous Green's function if one disregards all the terms proportional to  $\Theta' \sqrt{D/\hbar}$  and higher powers of this parameter. However, this contribution is nonzero only for the case of spin-dependent quasiparticle distribution. In the standard case of thermal spin-independent quasiparticle distribution the current is determined by the singlet component  $f_s$ . Consequently, it only contains the term proportional to the small factor  $e^{-d_F/\xi_F}$ . Certainly, the equilibrium Josephson current in the considered system contains the contribution generated by the LRTC, as it is well known<sup>1,2</sup>. If one calculates the current at the S/N boundary, then  $f_s$  should be modified by presence of LRTC and should contain a slowly decaying term, which provides the appropriate contribution. It is indeed the case for the system we consider. However, the corresponding term is proportional to  $(\Theta' \xi_F)^2$  and is disregarded in our calculation. Surely, it should be taken into account upon calculating the Josephson current for the case of spin-independent quasiparticle distribution, because in spite of the small factor  $(\Theta' \xi_F)^2$  it can result in large enough current contribution due to the absence of the suppression factor  $e^{-d_F/\xi_F}$ . At the same time we can safely disregard this term, because for the considered case of spin-dependent quasiparticle distribution the main contribution to the Josephson current is given by  $f_{LR}$  term, which contains neither  $(\Theta' \xi_F)^2$  nor the ferromagnetic suppression factor  $e^{-d_F/\xi_F}$ .

In order to generate a spin-dependent quasiparticle distribution in the interlayer, additional electrodes are attached to the normal regions of the interlayer. While in the paper we propose some particular way of such a distribution creation, it is not important how particularly it is obtained. The main point is to have a vector part  $\varphi(\varepsilon)$  of the distribution function in the interlayer, generated anyway. If this is the case, the discussed below results qualitatively survive.

In the present paper we assume that each of the normal regions of the interlayer is attached to two additional normal electrodes  $N_b^{l(r)}$  and  $N_t^{l(r)}$  (See Fig. 1). In their turn, the electrodes  $N_b^l$  and  $N_b^r$  have insertions  $P_l$  and  $P_r$  made of a strongly ferromagnetic material. Let the voltage  $V_b^{l(r)} - V_t^{l(r)} = V^{l(r)}$  is applied between the electrodes  $N_b^{l(r)}$  and  $N_t^{l(r)}$ . Here  $V_b^{l(r)}$  and  $V_t^{l(r)}$  are the electric potentials of the outer regions of the  $N_b^{l(r)}$  and  $N_t^{l(r)}$  electrodes with respect to the potential of the superconducting leads. It is worth to note here that the

superconductor is assumed to be closed to a loop and the voltage between the superconducting leads is absent. The conductances of the  $N^{l(r)}/N_b^{l(r)}$  and  $N^{l(r)}/N_t^{l(r)}$  interfaces are denoted by  $g_b^{l(r)}$  and  $g_t^{l(r)}$ , respectively.

Further, for definiteness we consider the left normal region of the interlayer with the corresponding additional electrodes. We choose the quantization axis  $z_l$  along the magnetization of the left ferromagnetic insertion  $P_l$  and the definitions  $R_{P_l\uparrow}$ ,  $R_{P_l\downarrow}$  stand for the  $P_l$  region resistivities for spin-up and spin-down electrons. Then under the conditions that (i) the  $N^l$  layer resistance  $R_N$  and the resistance of  $N_b^l$  region inclosed between  $N^l$  and  $P_l$  can be disregarded as compared to  $1/g_t$  and  $R_{P_l\downarrow}$  and (ii)  $1/R_{P_l\downarrow} \ll g_t^l \ll 1/R_{P_l\uparrow}$  one can believe that the voltage drops mainly at the  $P_l$  region for spin-down electrons and at the  $N^l/N_b^l$  interface for spin-up electrons. Also, the dissipative current flowing through  $N_b^l/N^l/N_t^l$  system is small and can be disregarded. We assume that the electron's spin relaxation is slow enough. Consequently, it is obtained that the electric potentials for spin-up and spin-down electrons in the  $N_b^l$  region inclosed between  $P_l$  and  $N^l$  are different and practically constant over this region. While the spin-up electrons are at the electric potential  $V_b^l$  in this region, the potential for spin-down electrons is approximately  $V_t^l$ .

In order to simplify the calculations we assume that  $V^l = V^r = V_b - V_t \equiv 2V$ . The left and the right additional electrodes only differ by the direction of the magnetization of the  $P_l$  and  $P_r$  insertions. For later use we define the unit vectors aligned with the  $P_l$  and  $P_r$  magnetizations as  $\mathbf{M}_l$  and  $\mathbf{M}_r$ , respectively. In order to satisfy the electroneutrality condition the electric potential of the superconducting leads should be equal to  $(V_t + V_b)/2$ . Then the electric potentials for spin-up and spin-down electrons in the  $N_b^l$  region inclosed between  $P_l$  and  $N^l$  counted from the level of the superconducting leads are  $V_\uparrow = (V_b - V_t)/2 = V$  and  $V_\downarrow = (V_t - V_b)/2 = -V$ . Due to the fact that one can disregard the voltage drop inside this region, the distribution functions for spin-up and spin-down electrons in this region are close to the equilibrium form (with different electrochemical potentials). For the general case (if the quantization axis does not aligned with the  $P_l$  magnetization) the distribution function becomes a matrix in spin space and takes the form

$$\hat{\varphi}_l = \varphi_0 \sigma_0 + \varphi_t \mathbf{M}_l \boldsymbol{\sigma},$$

$$\varphi_0 = \frac{1}{2} \left[ \tanh \frac{\varepsilon - eV}{2T} + \tanh \frac{\varepsilon + eV}{2T} \right],$$

$$\varphi_t = \frac{1}{2} \left[ \tanh \frac{\varepsilon - eV}{2T} - \tanh \frac{\varepsilon + eV}{2T} \right]. \quad (34)$$

The same form of the distribution function is valid for the  $N_b^r$  part enclosed between  $P_r$  and  $N^r$  with the substitution  $\mathbf{M}_r$  for  $\mathbf{M}_l$ .

Now we can obtain the distribution function in the  $N^l$  and  $N^r$  regions of the interlayer, which enters current (21). For the considered case  $g_t \ll 1$  the dissipative



current flowing through  $N_b^l/N_t^l/N_t^r$  junction is negligible and, therefore, the  $y$ -dependence of the distribution function in the  $N^{l(r)}$  region can be disregarded. Then under the condition  $\sigma_F \ll \sigma_N$  the distribution functions  $\tilde{\varphi}^{(0)}$  in the  $N^l$  and  $N^r$  regions calculated to the zero order in the S/N conductance  $\tilde{G}_T$  are spatially constant and equal to  $\hat{\varphi}_l$  and  $\hat{\varphi}_r$ , respectively. Indeed, the equation for the distribution function (22) at  $\mathbf{h} = 0$  and boundary conditions at S/N interfaces (24) (corresponding to  $G_\phi = 0$ ) are satisfied by this solution. Boundary conditions at F/N interfaces (23) are satisfied approximately due to the smallness of the distribution function gradient under the condition  $\sigma_F \ll \sigma_N$ .

Although the distribution function in the middle F layer does not enter the current expression (21), it is interesting to discuss here how it behaves. For simplicity we consider the limiting case  $\Theta' \rightarrow 0$ , when the exchange field in the ferromagnet is practically constant and the qualitative physical picture is more clear. According to Eq. (22) and boundary conditions (23) the scalar part of the distribution function  $\varphi_0$  is constant over the F layer and coincide with its value in the  $N^l$  and  $N^r$  regions. The vector component parallel to the exchange field of the ferromagnet is a linear function of  $x$ -coordinate, which matches the constant values  $\varphi_t \mathbf{M}_{l(r)} \mathbf{h}_{l(r)}/h$  at the F/N interfaces. Here  $\mathbf{h}_{l,r} \equiv \mathbf{h}(x = \mp d_F/2)$  are the exchange field values at the left and right N/F interfaces. The vector component perpendicular to the exchange field of the ferromagnet decays from the F/N interfaces into the ferromagnetic region at the characteristic length  $\xi_F$  oscillating simultaneously with a period  $2\pi\xi_F$ , as it can be obtained from Eq. (22) and boundary conditions (23). If one goes beyond the approximation  $\sigma_F/\sigma_N \ll 1$ , the distribution function in the  $N^l$  and  $N^r$  regions acquires gradient terms proportional to the parameter  $\sigma_F/\sigma_N$ . In order to calculate these terms correctly one needs to solve real two-dimensional problem involving the additional electrodes. While the solution of this problem is quite complicated, it does not influence qualitatively our main conclusions regarding the additional contributions to the current under the condition that the quasiparticle distribution is spin-dependent. For this reason we restrict our consideration by the case  $\sigma_F/\sigma_N \ll 1$ , when the distribution function (34) is a good approximation to the solution.

Now we turn to the discussion of the Josephson current through the junction. It is expressed by Eq. (21). As for the considered case of nonmagnetic S/N interfaces  $G_{MR} = 0$ , the last term in this formula is absent. Due to the fact that the scalar part  $\varphi_0^{(0)}$  of the distribution function in the interlayer [Eq. (34)] is an odd function of quasiparticle energy, the part of the current generated by the term  $\propto \cosh \Theta_S^R [\varphi_0^{(0)}(\varepsilon) + \varphi_0^{(0)}(-\varepsilon)]/2$  also vanishes. Further, in order to avoid the flowing of a quasiparticle current through the junction we assume that  $|eV| < \Delta$  and the temperature is low ( $T \ll \Delta$ ). Under these conditions the linear in  $x$ -coordinate part of  $\varphi^{(1)}$

(it is this term that provides the flowing of the quasiparticle current through the junction) is zero in each of the  $N$  regions of the interlayer, as it is dictated by boundary conditions (24). Therefore,  $\varphi^{(1)}$  is approximately constant in each of the  $N$  layers. We comment on the values of these constants below.

The first two terms in Eq. (21) represent the contribution of the SCDOS singlet part, which takes place as for the case of spin-independent quasiparticle distribution, so as when this distribution is spin-dependent. After substitution of the particular expressions for the singlet part of the anomalous Green's function [Eq. (25)] and the scalar part of the distribution function [Eqs. (34) and (20)] this contribution takes the form

$$j_s = \frac{G_T^2 \sin \chi}{8e\sigma_F} \int_{-\infty}^{\infty} \frac{i\Delta^2 d\varepsilon \tilde{\varphi}_0(\varepsilon)}{[(\varepsilon + i\delta)^2 - \Delta^2] \cosh^2 \phi_N} \times \left[ \frac{\cosh \phi_+}{\lambda_+ \sinh \phi_+ + \rho_N \cosh \phi_+} - \frac{\sinh \phi_+}{\lambda_+ \cosh \phi_+ + \rho_N \sinh \phi_+} + \frac{\cosh \phi_-}{\lambda_- \sinh \phi_- + \rho_N \cosh \phi_-} - \frac{\sinh \phi_-}{\lambda_- \cosh \phi_- + \rho_N \sinh \phi_-} \right]. \quad (35)$$

The third term in Eq. (21) contains the current flowing through the SCDOS triplet part and is nonzero only for the case of spin-dependent quasiparticle distribution. This contribution is the main result of the present section. If one substitutes the particular expressions for the triplet part of the anomalous Green's function [Eqs. (26),(27)] and the vector part of the distribution function [Eqs. (34) and (20)] this contribution takes the form

$$j_t^{l,r} = -j_{SR} \frac{\mathbf{h}_{l,r} \mathbf{M}_{l,r}}{h} + \alpha j_{LR} \frac{(\mathbf{M}_{l,r} \times \mathbf{h}_{l,r}) \mathbf{e}_x}{h}, \quad (36)$$

where  $\mathbf{e}_x$  is the unit vector along the  $x$ -direction. The currents  $j_{SR}$  and  $j_{LR}$  are generated by the short-range and long-range triplet components of the anomalous Green's function, respectively. Consequently, if the F layer is thick, that is  $\xi_F \lesssim d_F$ , the current  $j_{SR}$  is small due to the factor  $e^{-d_F/\xi_F}$ , while  $j_{LR}$  is not suppressed by this factor.

The expressions for currents  $j_{SR}$  and  $j_{LR}$  take the form

$$j_{SR} = -\frac{G_T^2 \sin \chi}{8e\sigma_F} \int_{-\infty}^{\infty} \frac{i\Delta^2 d\varepsilon \tilde{\varphi}_t(\varepsilon)}{[\Delta^2 - (\varepsilon + i\delta)^2] \cosh^2 \phi_N} \times \left[ \frac{\cosh \phi_+}{\lambda_+ \sinh \phi_+ + \rho_N \cosh \phi_+} - \frac{\sinh \phi_+}{\lambda_+ \cosh \phi_+ + \rho_N \sinh \phi_+} - \frac{\cosh \phi_-}{\lambda_- \sinh \phi_- + \rho_N \cosh \phi_-} + \frac{\sinh \phi_-}{\lambda_- \cosh \phi_- + \rho_N \sinh \phi_-} \right], \quad (37)$$

$$j_{LR} = -\frac{G_T^2 \sin \chi}{8e\sigma_F} \int_{-\infty}^{\infty} \frac{i\Delta^2 d\varepsilon \tilde{\varphi}_t(\varepsilon)}{[\Delta^2 - (\varepsilon + i\delta)^2] \cosh^2 \phi_N} \times$$

$$\left\{ \frac{\Theta' \cosh \phi_t}{\rho \cosh \phi_t + \lambda_t \sinh \phi_t} \left[ \frac{\sinh \phi_+}{\lambda_+ \cosh \phi_+ + \rho \sinh \phi_+} - \frac{\sinh \phi_-}{\lambda_- \cosh \phi_- + \rho \sinh \phi_-} \right] - \frac{\Theta' \sinh \phi_t}{\rho \sinh \phi_t + \lambda_t \cosh \phi_t} \left[ \frac{\cosh \phi_+}{\lambda_+ \sinh \phi_+ + \rho \cosh \phi_+} - \frac{\cosh \phi_-}{\lambda_- \sinh \phi_- + \rho \cosh \phi_-} \right] \right\}. \quad (38)$$

It is seen from Eq. (36) that the values of the current contribution  $j_t$  at the left and right S/N interfaces can be different, that is, in general,  $j_t^{l,r} = j_t \pm j_a$ . However, under the condition that the superconducting leads are closed into a loop the currents at the left and right S/N interfaces must be equal to each other. It appears that the distribution function in the N layers acquires additional terms  $\varphi_{l,r}^{(1)}$ , which are proportional to  $G_T$ . Under the condition  $V^l = V^r$  we obtain that  $\varphi_l^{(1)} = \varphi_r^{(1)}$ . Then, according to Eq. (21) this term results in the current contribution, which exactly compensates  $j_a$ . Therefore, the Josephson current  $j_t$  flowing through the junction can be simply calculated as  $j_t = (j_t^l + j_t^r)/2$ .

It is obvious from Eq. (34) that  $j_s$  is an even function of voltage  $V$  applied to the additional electrodes and  $j_t$  is an odd function of this voltage. Therefore, it is easy to extract in experiment contributions  $j_s$  and  $j_t$  from the full Josephson current:  $j_s(V) = (j(V) + j(-V))/2$ , while  $j_t(V) = (j(V) - j(-V))/2$ . Further, it is seen from Eq. (36) that by choosing the appropriate orientation of  $P_l$  and  $P_r$  magnetizations, one can, in principle, measure either  $j_{SR}$  or  $j_{LR}$  current contributions. For this reason it makes sense to discuss all the current contributions  $j_s$ ,  $j_{SR}$  and  $j_{LR}$  separately. In the tunnel limit all of them manifest sinusoidal dependence on the superconducting phase difference  $\chi$ , that is  $j_{s,SR,LR} = j_{s,SR,LR}^c \sin \chi$ . Therefore, we only discuss the corresponding critical currents  $j_s^c$ ,  $j_{SR}^c$ ,  $j_{LR}^c$  below.

Fig. 2 represents these contributions as a function of voltage  $V$ . First of all, it is worth to note that current components  $j_{SR}$  and  $j_{LR}$ , carried by the triplet part of SCDOS, are nonzero only for  $V \neq 0$ . That is, indeed, the triplet part of SCDOS only contributes to the current if a spin-dependent quasiparticle distribution is created in the interlayer. The exchange field  $h$  is chosen to be not very strong  $h = 10\Delta$ . Such a choice is in general agreement with the characteristic values of the exchange field in weak ferromagnetic alloys. However, the results discussed below qualitatively survive for the case of more strong exchange fields. Roughly speaking, increasing of the exchange field influences the results in the same manner as increasing of the  $F$  layer length  $d_F$ .

Panels (a), (b) and (c) correspond to different lengths of the  $N$  and  $F$  regions forming the interlayer. Below all

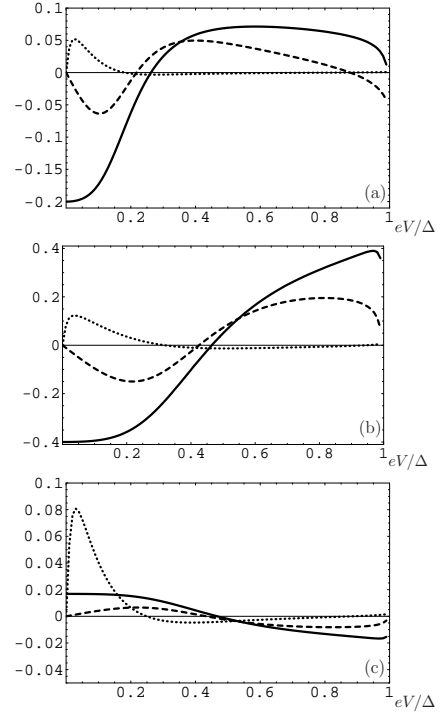


FIG. 2. Current components  $j_s^c$  (solid line),  $j_{SR}^c$  (dashed line) and  $j_{LR}^c$  (dotted line) as functions of voltage  $V$ , applied between the additional electrodes. The currents are measured in arbitrary units. Panel (a) corresponds to  $d_F = 1$ ,  $d_N = 2$ , for panel (b)  $d_F = 1$ ,  $d_N = 1$  and for panel (c)  $d_F = 2$ ,  $d_N = 1$ . All lengths are measured in units of  $\xi_S$ . The other parameters are the following:  $h = 10\Delta$ ,  $\Theta'\xi_S = 0.2$ ,  $T = 0$ .

the lengths are expressed in units of the superconducting coherence length  $\xi_S$ . The magnetic coherence length  $\xi_F = \xi_S \sqrt{\Delta/\hbar}$  is approximately three times shorter than  $\xi_S$ . For panels (a) and (b) the ferromagnetic layer is not thick ( $d_F = 1$ ). They differ by the length of the normal layer: panel (a) corresponds to  $d_N = 2$  and for panel (b)  $d_N = 1$ . As it is expected, upon increasing  $d_N$  the magnitude of all the current components decreases not very sharply. The corresponding decay length is considerably larger than  $\xi_F$ . On the contrary, increase of  $d_F$  suppresses current components  $j_s$  and  $j_{SR}$  exponentially with the characteristic decay length  $\xi_F$ . It is natural because they flow via the singlet and short-range triplet components of the anomalous Green's function. These components are composed of the Cooper pairs with opposite spin direction and, correspondingly, decay rapidly into the depth of the ferromagnetic region. It is seen from the figures that for panels (a) and (b)  $j_{SR}$  and  $j_{LR}$  are of the same order, while  $j_s$  is even larger. This is not the case for panel (c), where  $d_F = 2$ . For this parameter range  $j_s$  and  $j_{SR}$  are already suppressed. However, for a certain voltage range (small enough voltages)  $j_{LR}$  is not suppressed and the dependence of its magnitude on  $d_F$  is the same as on  $d_N$ . For larger voltages the value of  $j_{LR}$  is also suppressed. It is interesting to note that this sup-

pression takes place for all the panels of Fig. 2 irrespective of the  $F$  layer length. It is obvious that the insensitivity of  $j_{LR}$  to the length of the ferromagnetic region is a result of the fact that it is carried by Cooper pairs composed of the electrons with parallel spins. However, the characteristic behavior of this component in dependence on  $V$  (sharp maximum at small voltages and subsequent suppression) requires an additional explanation. Such an explanation is closely connected to the particular shape of the anomalous Green's function LRTC and is given below upon discussing the LRTC.

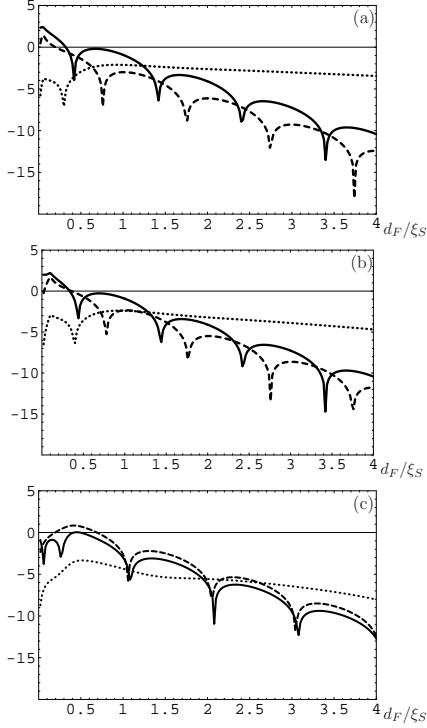


FIG. 3. Current components  $j_s^c$  (solid line),  $j_{SR}^c$  (dashed line) and  $j_{LR}^c$  (dotted line) in dependence on  $d_F/\xi_S$  (logarithmic scale). Panel (a) corresponds to  $V = 0.05\Delta$ ,  $V = 0.1\Delta$  for panel (b) and  $V = 0.5\Delta$  for panel (c). The other parameters are the following:  $h = 10\Delta$ ,  $\Theta'\xi_S = 0.2$ ,  $d_N = 1$ ,  $T = 0$ .

Further, the dependence of all three current components on the length of the ferromagnetic layer is studied in more detail. Panels (a), (b) and (c) of Fig. 3 demonstrate this dependence for three different voltages  $V$ . For panel (a) the particular value of this voltage is chosen to be  $V = 0.05\Delta$ . This value approximately corresponds to the maximum of  $j_{LR}$  in Fig. 2. For panel (b)  $V = 0.1\Delta$ . Current  $j_{LR}$  gradually declines at this voltage region. Finally, the plots shown in panel (c) correspond to  $V = 0.5\Delta$ , where  $j_{LR}$  is already greatly suppressed. First of all, it is worth to note that the decay length of  $j_s$  and  $j_{SR}$  is  $\xi_F$  to a good accuracy for any voltage region. Also, it is seen from Fig. 3 that  $j_s$  and  $j_{SR}$  oscillate upon increasing  $d_F$  with the period  $2\pi\xi_F$  (irrespective of the particular voltage). For  $j_s$ , which is non-zero even for spin-independent quasiparticle distribution, these oscilla-

tions are well-studied. They are a hallmark of mesoscopic LOFF-state, as it was mentioned in the introduction.  $j_{SR}$  is absent for spin-independent quasiparticle distribution, but is carried by the same pairs of electrons with opposite spin directions, just as  $j_s$ , and, consequently, also manifests the LOFF-state oscillations. While the oscillation period is the same for  $j_s$  and  $j_{SR}$ , there is a phase shift between their oscillations, which depends on the particular value of the voltage  $V$ .

Unlike  $j_s$  and  $j_{SR}$ ,  $j_{LR}$  does not manifest oscillating behavior. Its decay length is not connected to  $\xi_F$  and crucially depends on  $V$ . This decay length  $l_{LR}$  is maximal for the voltage region, where  $j_{LR}$  has maximal value ( $l_{LR} \approx 2\xi_S \approx 6\xi_F$  for panel (a)) and declines upon increasing  $V$ .

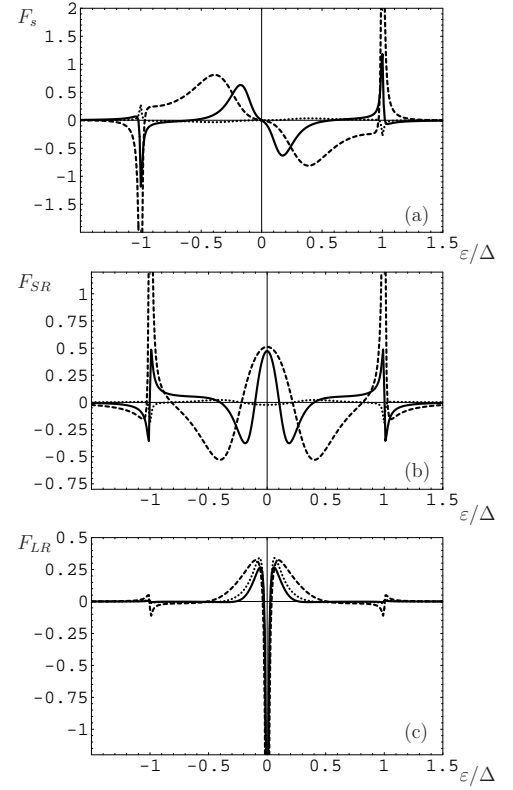


FIG. 4. Combinations  $F_s$  [panel(a)],  $F_{SR}$  [panel (b)] and  $F_{LR}$  [panel (c)] as functions of quasiparticle energy  $\epsilon/\Delta$ . In each panel ( $d_F = 1$ ,  $d_N = 2$ ) for solid curves, ( $d_F = 1$ ,  $d_N = 1$ ) for dashed curves and ( $d_F = 2$ ,  $d_N = 1$ ) for dotted curves. The other parameters are the same as in Fig. 2.

As it was already mentioned in the introduction, the dependence of the anomalous Green's function in the interlayer on the quasiparticle energy can be partially extracted from the Josephson current measurements. It can be done due to the fact that voltage  $V$  enters the current expression (21) only via distribution function (34). Then, according to Eqs. (21), (36) and (26), by taking the derivatives of the Josephson currents  $j_s$ ,  $j_{SR}$  and  $j_{LR}$  with respect to the voltage applied between the addi-

tional electrodes, at  $T \rightarrow 0$  one obtains that

$$\begin{aligned} dj_s/dV &\sim \text{Im} \left[ \frac{f_s^r(V)}{\sqrt{\Delta^2 - (eV + i\delta)^2}} \right], \\ dj_{SR}/dV &\sim \text{Im} \left[ \frac{f_{SR}^r(V)}{\sqrt{\Delta^2 - (eV + i\delta)^2}} \right], \\ dj_{LR}/dV &\sim \text{Im} \left[ \frac{f_{LR}^r(V)}{\sqrt{\Delta^2 - (eV + i\delta)^2}} \right]. \end{aligned} \quad (39)$$

Here  $f_{SR}^r$ ,  $f_{LR}^r$  and  $f_s^r$  are determined by Eqs. (28), (30) and (32), respectively. That is, indeed, imaginary parts of the anomalous Green's function components coming from the opposite interface corresponding to all three types of superconducting correlations, induced by the proximity effect in the interlayer, can be extracted from the Josephson current measurements. However, under the condition  $|eV| < \Delta$  it can be done only for subgap energies  $|\varepsilon| < \Delta$ . It is worth to note here that the derivatives of current components  $j_s$ ,  $j_{SR}$  and  $j_{LR}$  with respect to  $V$  give us the corresponding anomalous Green's function components only in the tunnel limit  $\tilde{G}_T \ll 1$ . In general case these derivatives are proportional to the appropriate components of SCDOS, which are expressed via the anomalous Green's function in a more complicated way.

Panels (a), (b) and (c) of Fig. 4 represent combinations  $F_s \equiv \text{Im} [f_s^r(\varepsilon)/\sqrt{\Delta^2 - (\varepsilon + i\delta)^2}]$ ,  $F_{SR} \equiv \text{Im} [f_{SR}^r(\varepsilon)/\sqrt{\Delta^2 - (\varepsilon + i\delta)^2}]$  and  $F_{LR} \equiv \text{Im} [f_{LR}^r(\varepsilon)/\sqrt{\Delta^2 - (\varepsilon + i\delta)^2}]$ , respectively, in dependence on quasiparticle energy  $\varepsilon$  measured in units of  $\Delta$ . In each panel different curves correspond to different lengths  $d_N$  and  $d_F$  (See caption to Fig. 4). It is seen that the value of the normal region length does not influence qualitatively all three components of the anomalous Green's function. As it is expected,  $F_s$  and  $F_{SR}$  are strongly suppressed upon increasing of  $d_F$ . On the contrary,  $F_{LR}$  is only very weakly sensitive to changing of  $d_F$ . It is dominated by the sharp dip at low energies, which followed by wider peaks, where  $F_{LR}$  changes sign. The width  $\delta\varepsilon$  of the dip is  $\sim \sqrt{\Delta D \Theta'}$ .

The characteristic shape of  $F_{LR}$  is responsible for  $j_{LR}$  behavior in dependence on  $V$ , shown in Fig. 2. The point is that at low enough temperatures only the part of  $F_{LR}$ , belonging to energy interval  $[-|eV|, |eV|]$ , contributes to  $j_{LR}$ . Consequently, upon increasing of  $V$   $j_{LR}$  grows sharply up to  $V \sim (1/2)\sqrt{\Delta D \Theta'}$  and after that starts to decline due to the opposite sign contribution of the peaks. It appears that the contributions of the dip and the peaks mainly compensate each other, what leads to strong suppression of  $j_{LR}$  for large enough  $V$ . The discussed above dependence of  $j_{LR}$  decay length on  $V$  is also closely connected to the fact that only the part of  $F_{LR}$ , belonging to energy interval  $[-|eV|, |eV|]$ , "works" upon creating  $j_{LR}$ . Indeed, it can be seen from Eq. (38) that the characteristic decay length of  $F_{LR}(\varepsilon)$   $d_F^c(\varepsilon) \sim |\lambda_t(\varepsilon)|^{-1}$ . There-

fore,  $j_{LR}$  decay length  $\sim 1/\Theta'$  for small voltages and gets shorter for larger voltages due to increased contribution of higher energies.

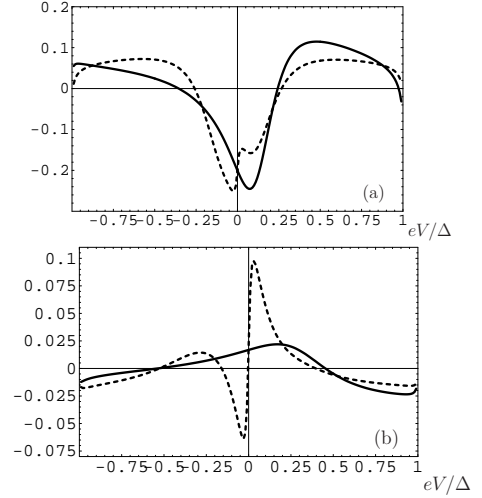


FIG. 5. Joint currents  $j_s^c + j_{SR}^c$  (solid curves) and  $j_s^c + j_{LR}^c$  (dashed curves) as functions of  $eV/\Delta$ . For panel (a)  $d_F = 1$ ,  $d_N = 2$  and for panel (b)  $d_F = 2$ ,  $d_N = 1$ . The other parameters are the same as in Fig. 2.

The possibility to extract singlet and triplet components of the proximity-induced anomalous Green's function in the interlayer is not the only motivation to study the Josephson current under spin-dependent quasiparticle distribution. Being an easily controllable parameter, voltage  $V$  gives a possibility to obtain highly nonlinear characteristics  $j(V)$  with a number of  $0-\pi$  transitions, which can be essential for superconducting electronics. As it was already mentioned above, by choosing the appropriate orientation of  $P_l$  and  $P_r$  magnetizations, one can, in principle, "turn off" either  $j_{SR}$  or  $j_{LR}$  current contribution. When the full current through the junction is given by joint contribution of  $j_{LR}$  and  $j_s$  or  $j_{SR}$  and  $j_s$ , respectively. The corresponding full currents are demonstrated in Fig. 5. Panel (a) represents the case of short enough ferromagnetic layer  $d_F = 1$ , while panel (b) corresponds to  $d_F = 2$ . It is seen from panel (b) that in this case the main contribution to the current is given by  $j_{LR}$ , at least for small enough voltages. It is worth to note that it may be not easy to adjust  $P_l$  and  $P_r$  magnetizations in such a way that only one of the components  $j_{SR}$  and  $j_{LR}$  flows. In fact, it is not necessary in order to obtain highly nonlinear  $j(V)$  characteristics. For this purpose it is enough to create any spin-dependent quasiparticle distribution in the interlayer region. The internal structure of the anomalous Green's function  $F_{LR}$  can also be studied separately with the help of arbitrary spin-dependent distribution for long enough ferromagnetic interlayers.

#### IV. S/N/S JUNCTION WITH MAGNETIC INTERFACES

In this section Josephson current is studied for S/N/S junction with magnetic S/N interfaces under the condition of spin-dependent quasiparticle distribution in the interlayer. The model is already described in Sec. II. The anomalous Green's function in the interlayer is found to the first order in S/N conductance  $\tilde{G}_T$  and spin-filtering parameter  $\tilde{G}_{MR}$  according to Eqs. (14) and (16) (assuming  $\mathbf{h} = 0$ ). In general, the condensate penetrating into the interlayer region is comprised of two types of electron pairs: with opposite electron spins and with parallel electron spins. However, due to the absence of ferromagnetic elements in the interlayer region they have the same characteristic decay length. The both types of pairs occur in the system if there is a reason for spin-flip there. For example, it is the case if the magnetization vectors of the both interfaces are not parallel  $\mathbf{m}_l \nparallel \mathbf{m}_r$ . If  $\mathbf{m}_l \parallel \mathbf{m}_r$ , then only the pairs with opposite electron spins, generated by the singlet superconductor, occur in the interlayer region. In order to make the formulae less cumbersome we give final expressions only for the case  $\mathbf{m}_l \parallel \mathbf{m}_r \equiv \mathbf{m}$ . Then, at the left ( $\alpha = +1$ ) and right ( $\alpha = -1$ ) S/N interfaces the singlet part of the anomalous Green's function takes the following form

$$\begin{aligned} f_s^R &= f_{s1} e^{-i\alpha\chi/2} + f_{s2} e^{i\alpha\chi/2} , \\ f_{s1} &= \frac{2i\pi G_T \sinh \Theta_S^R}{\sigma_N Z} \left[ \lambda_N + \frac{1}{\lambda_N} \left( \frac{G_\phi}{\sigma_N} \right)^2 \right] \sinh[2\lambda_N d_N] , \\ f_{s2} &= \frac{4i\pi G_T \sinh \Theta_S^R}{\sigma_N Z} \left[ \lambda_N - \frac{1}{\lambda_N} \left( \frac{G_\phi}{\sigma_N} \right)^2 \right] \sinh[\lambda_N d_N] , \\ Z &= 4\lambda_N^2 \sinh^2[\lambda_N d_N] + 8 \left( \frac{G_\phi}{\sigma_N} \right)^2 (\cosh^2[\lambda_N d_N] + 1) + \\ &\quad 4 \left( \frac{G_\phi}{\sigma_N} \right)^4 \frac{\sinh^2[\lambda_N d_N]}{\lambda_N^2} , \end{aligned} \quad (40)$$

where  $\lambda_N$  is determined below Eq. (25).

The triplet component of the anomalous Green's function has only  $z$ -component and takes the form

$$\begin{aligned} \mathbf{f}_t^R &= (0, 0, f_z) , \\ f_z &= f_{z1} e^{-i\alpha\chi/2} + f_{z2} e^{i\alpha\chi/2} , \\ f_{z1} &= \frac{4\pi G_\phi G_T \sinh \Theta_S^R}{\sigma_N^2 Z} \times \\ &\quad \left( \left[ 1 + \frac{1}{\lambda_N^2} \left( \frac{G_\phi}{\sigma_N} \right)^2 \right] \sinh^2[\lambda_N d_N] + 2 \right) , \\ f_{z2} &= \frac{8\pi G_\phi G_T \sinh \Theta_S^R}{\sigma_N^2 Z} \cosh[\lambda_N d_N] , \end{aligned} \quad (41)$$

where  $Z$  is determined in Eq. (40). Physically,  $f_{s,z1}$  is generated by the proximity effect at the same S/N interface and  $f_{s,z2}$  is extended from the opposite S/N interface.

Just as in the previous section, in order to generate a spin-dependent quasiparticle distribution in the interlayer, additional electrodes are attached to it. The principal scheme is the same as before except for the fact that there is only one normal region in the considered system. Therefore, we assume that the interlayer is attached to two additional normal electrodes  $N_b$  and  $N_t$  and electrode  $N_b$  has insertion  $P$  made of a strongly ferromagnetic material. The unit vector aligned with the magnetization of  $P$  is denoted by  $\mathbf{M}$ . Again, if voltage  $2V$  is applied between the electrodes  $N_b$  and  $N_t$ , then the electric potentials for spin-up and spin-down electrons in the  $N_b$  region, inclosed between  $P$  and the normal interlayer, counted from the level of the superconducting leads are  $V_\uparrow = (V_b - V_t)/2 = V$  and  $V_\downarrow = (V_t - V_b)/2 = -V$ . The distribution functions for spin-up and spin-down electrons in this region are close to the equilibrium form (with different electrochemical potentials). In a matrix form the distribution function is expressed by Eq. (34) with the substitution  $\mathbf{M}$  for  $\mathbf{M}_l$ .

Now we can obtain the distribution function in the interlayer, which enters the current (21). Again, for simplicity we assume that  $g_t \ll 1$ . Consequently, the dissipative current flowing through  $N_b/N/N_t$  junction is negligible and, therefore, the  $y$ -dependence of the distribution function in the interlayer region can be disregarded. For simplicity we assume below that  $\mathbf{M} \parallel \mathbf{m}_l \parallel \mathbf{m}_r$ . Under this condition the distribution function  $\hat{\varphi}^{(0)}$  in the interlayer calculated according to Eq. (22) at  $\mathbf{h} = 0$  supplemented by boundary conditions at S/N interfaces (24) is spatially constant and equal to its value coming from  $N_b$  region. If  $\mathbf{M} \nparallel \mathbf{m}$ , then the spatially constant distribution function does not satisfy boundary conditions (24) any more. In this case the problem become two-dimensional and much more complicated.

Now we are able to calculate the Josephson current through the junction according to Eq. (21). After substitution of the expression for the singlet part of the anomalous Green's function [Eq. (40)] and the scalar part of the distribution function [Eqs. (34) and (20)] into first two terms of Eq. (21), the contribution of the SCDOS singlet part takes the form

$$\begin{aligned} j_s &= \frac{2iG_T^2 \sin \chi}{e\sigma_N} \int_{-\infty}^{\infty} \Delta^2 d\varepsilon \tilde{\varphi}_0(\varepsilon) \times \\ &\quad \frac{\lambda_N \sinh[\lambda_N d_N] (1 - \left[ \frac{G_\phi}{\sigma_N \lambda_N} \right]^2)}{[(\varepsilon + i\delta)^2 - \Delta^2] Z(\varepsilon)} , \end{aligned} \quad (42)$$

where  $Z(\varepsilon)$  is determined in Eq. (40).

The current flowing through the SCDOS triplet part and expressed by the third term in Eq. (21) takes the form (in order to obtain this expression one should sub-

stitute Eqs. (41), (34) and (20) into Eq. (21))

$$j_t = \frac{4G_T^2 G_\phi \sin \chi}{e\sigma_N^2} \int_{-\infty}^{\infty} \Delta^2 d\varepsilon \tilde{\varphi}_t(\varepsilon) \times \frac{\cosh[\lambda_N d_N] \left(1 - \left[\frac{G_\phi}{\sigma_N \lambda_N}\right]^2 \frac{1 - \sinh[\lambda_N d_N]}{\sinh[\lambda_N d_N]}\right)}{[(\varepsilon + i\delta)^2 - \Delta^2] Z(\varepsilon)}. \quad (43)$$

As opposed to the problem of S/NFN/S junction considered in the previous section, it is seen from Eq. (43) that  $j_t$  values at the left and right S/N interfaces are equal to each other. As for the case of S/NFN/S junction, the part of current (21) generated by the term  $\propto \cosh \Theta_S^R [\varphi_0^{(0)}(\varepsilon) + \varphi_0^{(0)}(-\varepsilon)]/2$  vanishes due to the fact that the scalar part  $\varphi_0^{(0)}$  of the distribution function in the interlayer [Eq. (34)] is an odd function of quasiparticle energy. Further, under the conditions  $|eV| < \Delta$  and  $T \ll \Delta$  the last term, generated by  $\propto \alpha G_{MR} \cosh \Theta_S^R \mathbf{m} [\varphi^{(0)}(\varepsilon) + \varphi^{(0)}(-\varepsilon)]/2$  also vanishes because this expression is an odd function of quasiparticle energy at  $|\varepsilon| < \Delta$  and is absent elsewhere. Taking into account that  $\mathbf{m}_l || \mathbf{m}_r || \mathbf{M}$  one can obtain from Eq. (24) that  $\partial_x \hat{\varphi}^{(1)} = 0$  at the S/N interfaces. Therefore,  $\hat{\varphi}^{(1)}$  is approximately constant in the interlayer. Moreover, this constant is to be equal to zero in order to satisfy the condition  $j^l = j^r$ . Therefore, the full Josephson current flowing through the junction is given by the sum of singlet [Eq. (42)] and triplet [Eq. (43)] SCDOS contributions.

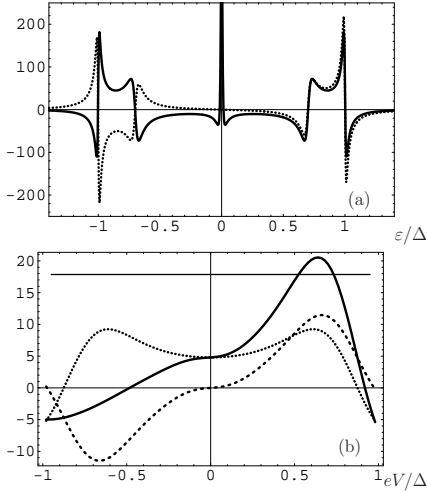


FIG. 6. (a) Functions  $F_s$  (dotted line) and  $F_t$  (solid line) as functions of  $\varepsilon/\Delta$  for S/N/S junction with magnetic interfaces. (b) Full critical current (solid line) and its contributions  $j_s$  (dotted line) and  $j_t$  (dashed line) as functions of  $eV/\Delta$ . For the both panels  $d_N = 0.5\xi_S$ ,  $G_\phi\xi_S/\sigma_N = 0.35$  and  $T = 0.1\Delta$ .

As for the previous case of S/NFN/S junction,  $j_s^c$  is an even function of voltage  $V$  applied to the additional electrodes and  $j_t^c$  is an odd function of this voltage. Therefore, contributions  $j_s^c$  and  $j_t^c$  can be extracted from an

experimentally measurable Josephson current and, so, it makes sense to discuss them separately. Panel (b) of Fig. 6 demonstrates the full critical Josephson current and its contributions  $j_s^c$  and  $j_t^c$  as functions of  $V$  for a typical set of parameters (See caption to Fig. 6 for specific values). Functions  $F_s(\varepsilon) \equiv \text{Im} [f_{s2}(\varepsilon)/\sqrt{\Delta^2 - (\varepsilon + i\delta)^2}]$  and  $F_t(\varepsilon) \equiv \text{Im} [f_{z2}(\varepsilon)/\sqrt{\Delta^2 - (\varepsilon + i\delta)^2}]$  are represented in panel (a) of Fig. 6 for the same set of parameters. As it is seen from the definitions given in Eqs. (40) and (41), these functions are proportional to the singlet and triplet components of the anomalous Green's function, coming from the opposite S/N interface, and can be experimentally found by differentiating the currents  $j_s^c$  and  $j_t^c$  with respect to voltage  $V$ , as it was explained in the previous section.

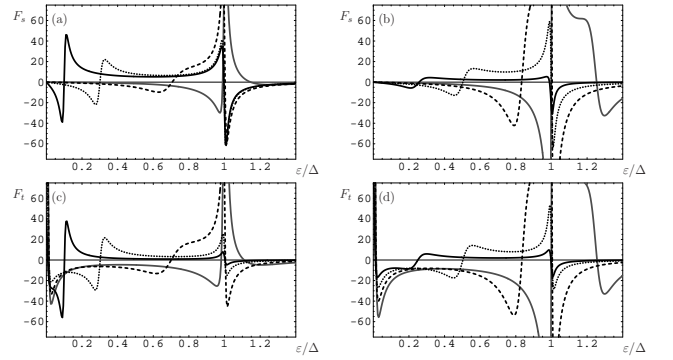


FIG. 7.  $F_s$  and  $F_t$  as functions of  $\varepsilon/\Delta$  for S/N/S junction with magnetic interfaces. The upper row represents  $F_s$ , while the lower row demonstrates  $F_t$ . For panels (a) and (c)  $d_N = \xi_S$  and different curves correspond to different values of  $G_\phi\xi_S/\sigma_N = 0.1$  (black solid curve), 0.3 (dotted curve), 0.7 (dashed curve) and 1.1 (gray solid curve). In panels (b) and (d)  $G_\phi\xi_S/\sigma_N = 0.5$  and different curves correspond to different  $d_N/\xi_S = 2$  (black solid curve), 1 (dotted curve), 0.6 (dashed curve) and 0.4 (gray solid curve).  $T = 0.1\Delta$ .

The characteristic shape of  $F_s$  and  $F_t$  dictates how  $j_s$  and  $j_t$  behave in dependence on  $V$ . Upon discussing the characteristic features of  $j_s$  and  $j_t$  we only consider  $V > 0$  and, correspondingly,  $\varepsilon > 0$  for  $F_s$  and  $F_t$ . The main characteristic features of  $F_s$  and  $F_t$ , which are responsible for the current behavior, are proximity induced dips at  $\varepsilon_\phi \sim G_\phi\xi_S^2\Delta/\sigma_N d_N$  (for the parameter region  $\varepsilon_\phi < \Delta$ ). These dips are followed by abrupt changing of sign of the corresponding quantity. Fig. 7 shows  $F_s$  and  $F_t$  evolution with  $G_\phi$  (left column) and with  $d_N$  (right column). It is seen that upon  $G_\phi$  increasing the proximity induced dip moves to higher energies. If the junction becomes shorter the dip also moves to the right and its integral height increases due to the fact that the proximity effect is more pronounced for short junctions. However, the described picture is only valid for  $G_\phi d_N/\sigma_N \lesssim 1$ . For larger values of  $G_\phi d_N/\sigma_N$  nonlinear effects generated by this parameter come into play and the proximity induced structures of  $F_t$  are substantially modified. Two symmet-



ric dips located at  $\varepsilon_\phi$  transform into a wide common dip and the energy locations where  $F_t$  changes sign are gradually shifted to lower energies. At the same time  $F_s$  does not manifest any qualitative changes upon increasing of this parameter. It is seen from panels (c) and (d) of Fig. 7 that  $F_t$  exhibits a narrow peak at zero energy. It is closely connected to the broadening parameter  $\delta$ . Its functional form is described as  $\propto \text{Re}[(\delta - i\varepsilon)^{-3/2}]$ .

According to Eqs. (21) and (34) at low enough temperatures only the part of  $F_s$ , belonging to energy intervals  $[-\infty, -|eV|]$  and  $[|eV|, +\infty]$ , contributes to  $j_s^c$ . Consequently, upon increasing of  $V$  the absolute value of  $j_s^c$  grows up to  $V \sim \varepsilon_\phi$  and after that starts to decline due to the sign changing of  $F_s(\varepsilon)$  at  $\varepsilon = \varepsilon_\phi$ . Analogously, only the part of  $F_t$ , belonging to energy interval  $[-|eV|, |eV|]$ , contributes to  $j_t^c$ . Therefore, the absolute value of  $j_t^c$  also grows up to  $V \sim \varepsilon_\phi$  and declines after that. The described behavior is characteristic for the absolute value of  $j_s^c$  and  $j_t^c$  as for  $eV > 0$ , so as for  $eV < 0$ . However, due to the fact that  $j_s^c$  is symmetric and  $j_t^c$  is antisymmetric function of  $V$ , the total Josephson current is highly non-symmetric with respect to  $V$ , as it is seen in Figs. 6 and 8. While for  $eV < 0$  the contributions of  $j_s^c$  and  $j_t^c$  partially compensate each other leading to suppression of the full current and  $0 - \pi$ -transition at some finite  $V$ , they are added for  $eV > 0$  resulting in the considerable current enhancement. The value of  $eV$ , where the peak in the critical current is located, can be used for experimental estimate of spin-mixing parameter  $G_\phi$ , characterizing the magnetic interface, because  $eV_p \sim \varepsilon_\phi$ . For short enough junctions with  $d_N < \xi_S$  the current value can even exceed the critical current value for S/N/S junction with nonmagnetic S/N interfaces ( $G_\phi = 0$ ) and the same S/N interface conductance  $G_T$  for some voltage range. It is worth to note here that such an enhancement is only possible for finite  $V$ , when the triplet part of SCDOS  $F_t$  contributes to the current. At  $V = 0$  the critical Josephson current through S/N/S junction with magnetic interfaces  $G_\phi \neq 0$  is always lower than the corresponding current for S/N/S junction with nonmagnetic interfaces but the same interface conductance  $G_T$  (this statement is valid for the entire range of parameters we consider).

Let us denote the value of the critical current for S/N/S junction with nonmagnetic interfaces and interface conductance  $G_T$  by  $j_{nm}(V)$ . The value  $j_{nm}(V = 0)$  is shown in Fig. 6(b) by the horizontal line. It is seen that a small excess of the total current  $j^c$  over  $j_{nm}(V = 0)$  takes place for some voltage range. However, the excess can be much greater, the current at finite  $V$  can exceed the equilibrium current  $j_{nm}(V = 0)$  for nonmagnetic S/N/S junction more than twice. Such a case is illustrated in Fig. 8(a). Maximal excess can be expected for short junctions with  $\varepsilon_\phi \approx \Delta$ , where the proximity effect in  $F_t$  is most pronounced and the proximity induced dip at  $\varepsilon_\phi$  merges with the coherence peak at  $\Delta$  thus greatly enhancing  $F_t$  value in the subgap region. In addition the temperature should be low enough in order to avoid temperature smearing of the effect.

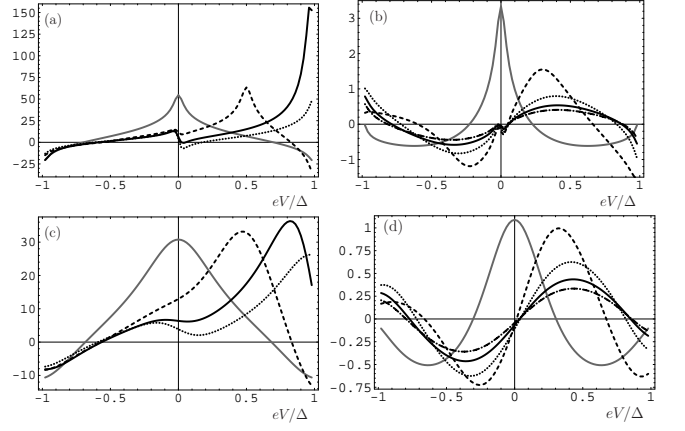


FIG. 8. Full critical Josephson current for S/N/S junction with magnetic interfaces in dependence on  $eV/\Delta$ . Panel (a) demonstrates the case of low-temperature junction, where the proximity effect is well-pronounced:  $T = 0.01\Delta$ ,  $d_N = 0.3\xi_S$ .  $G_\phi\xi_S/\sigma_N = 0.15$ (dashed curve),  $0.3$  (solid curve) and  $0.45$  (dotted curve). Panel (b) corresponds to longer junction at the same temperature:  $T = 0.01\Delta$ ,  $d_N = 3\xi_S$ .  $G_\phi\xi_S/\sigma_N = 1$ (dashed curve),  $2$  (dotted curve),  $3$  (solid curve) and  $4$  (dashed-dotted curve). Panels (c) and (d) represent the same results as panels (a) and (b), respectively, but at higher temperature  $T = 0.1\Delta$ . For all the panels the gray solid line represents  $j_{nm}(V)$  for the corresponding set of the parameters.

For longer junctions with  $d_N \gtrsim \xi_S$  the current does not exceed the equilibrium value  $j_{nm}(V = 0)$  because of weaker proximity effect in the interlayer region, as it is illustrated in Fig. 8(b). For all the panels of Fig. 8 the gray solid line represents  $j_{nm}(V)$  for the corresponding set of the parameters. It is worth to note here that dependencies  $j_{nm}(V)$  on  $V$  are qualitatively very similar to the current discussed in Ref. 30 for nonmagnetic S/N/S junction under nonequilibrium quasiparticle distribution in the normal interlayer. Indeed, at  $G_\phi = 0$  triplet part of SCDOS  $F_t$  is absent and, consequently, the vector part of the distribution function (34) does not contribute to the current. The singlet part of this distribution function is formally equivalent to the nonequilibrium distribution<sup>30</sup> for a narrow normal interlayer (a wire or a constriction). Full quantitative agreement between our results for  $j_{nm}(V)$  and the results of Ref. 30 cannot be reached because they are obtained for somewhat different parameter ranges.

Panels (c) and (d) of Fig. 8 show the results for the current at higher temperature  $T = 0.1\Delta$ . Panel (c) corresponds to shorter junction with  $d_N = 0.3\xi_S$ , while panel (d) demonstrates the case of longer junction with  $d_N = 3\xi_S$ . It is seen that for short junction, where the effect of current enhancement is well pronounced at low temperatures, raising of the temperature suppresses the effect. The reason is that distribution function (34) smears upon raising of the temperature. Consequently, not only the part of  $F_t$  corresponding to  $|\varepsilon| < \varepsilon_\phi$ , but

also some region of higher energies, where  $F_t$  has opposite sign, is involved into the current  $j_t$  now. This leads to partial compensation of  $F_t$  parts with different signs.

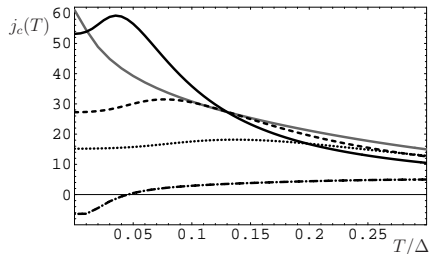


FIG. 9. Full critical Josephson current for S/N/S junction with magnetic interfaces in dependence on temperature for several different voltages  $V$ .  $d_N = 0.3\xi_S$ , black solid curve:  $G_\phi\xi_S/\sigma_N = 0.3$ ,  $eV/\Delta = 0.85$ ; dashed curve:  $G_\phi\xi_S/\sigma_N = 0.3$ ,  $eV/\Delta = 0.7$ ; dotted curve:  $G_\phi\xi_S/\sigma_N = 0.3$ ,  $eV/\Delta = 0.5$ ; dashed-dotted curve:  $G_\phi\xi_S/\sigma_N = 0.45$ ,  $eV/\Delta = 0.05$ . Gray solid curve represents the temperature dependence of  $j_{nm}(V = 0)$  for the corresponding set of parameters.

Although the maximal value of the critical Josephson current, which can be reached at a finite  $V$ , is suppressed by temperature, the current dependence on  $T$  at a particular voltage  $V$  can be quite interesting. Fig. 9 demonstrates how the current depends on temperature at several specified values of voltage  $V$  for the case of short junction with  $d_N = 0.3\xi_S$ . The gray solid line represents the dependence of  $j_{nm}(V = 0)$  on temperature and is given for comparison of our results with the equilibrium nonmagnetic case. It is well known, that the Josephson current for equilibrium nonmagnetic S/N/S junction declines upon raising of temperature rather sharply, as it is demonstrated by the gray solid curve. On the contrary, the current at finite  $V$  for a S/N/S with magnetic interfaces can even grow up to some temperature and only after that start to decline. The qualitative explanation of this fact is the following. The main contribution to the Josephson current in nonmagnetic equilibrium S/N/S junction is given by high peak of SCDOS located at low energies. Consequently, the temperature smearing of the equilibrium distribution function  $\tanh \varepsilon/2T$  crucially reduces the current. At the same time, the main contribution to  $j_t$  is given by the energies up to  $\varepsilon \sim |eV|$  and under the condition that  $|eV| < \varepsilon_\phi$  the temperature smearing of the distribution function involves higher energies, where the absolute value of  $F_t$  even larger, in the current transfer. In addition, at low voltages the junction can manifest  $0 - \pi$  transition in dependence on temperature.

## V. SUMMARY

In conclusion, we have theoretically investigated the Josephson current in weak links, containing ferromag-

netic elements, under the condition that the quasiparticle distribution in the weak link region is spin-dependent. Two types of weak link are considered. The first system is a S/N/F/N/S junction with complex interlayer composed of two normal metal regions and a middle layer made of a spiral ferromagnet, sandwiched between them. The second considered system is a S/N/S junction with magnetic S/N interfaces. In both cases spin-dependent quasiparticle distribution in the interlayer region is proposed to be created by attachment of additional electrodes with ferromagnetic elements to the interlayer region and applying a voltage  $V$  between them. Interplay of the triplet superconducting correlations, induced in the interlayer by the proximity with the superconducting leads, and spin-dependent quasiparticle distribution results in the appearance of the additional contribution to the Josephson current  $j_t$ , carried by the triplet part of SCDOS.

It is shown that  $j_t$  is an odd function of  $V$ , while the standard contribution  $j_s$ , carried by the singlet part of SCDOS, is an even function. So,  $j_t$  can be extracted from the full Josephson current measured as a function of  $V$ . Further, it is demonstrated that derivative  $dj_t/dV$  can provide direct information about the anomalous Green's function describing the superconducting triplet correlations induced in the interlayer. We show that in the S/N/F/N/S junction the contributions given by the short-range (SRTC) and long-range (LRTC) components of triplet superconducting correlations in the interlayer can be measured separately.

For S/N/S junction with magnetic interfaces it is also obtained that the critical Josephson current at some finite  $V$  can considerably exceed the current flowing through the equilibrium nonmagnetic S/N/S junction with the same S/N interface transparency. This enhancement is due to the fact that the triplet component of SCDOS "works" under spin-dependent quasiparticle distribution giving the additional contribution to the current, while it does not take part in the current transfer for spin-independent quasiparticle distribution. In addition, we have studied temperature dependence of the critical current in S/N/S junction with magnetic S/N interfaces. As opposed to the case of equilibrium nonmagnetic S/N/S junction, where the current is monotonously suppressed by temperature, in the considered case at a finite voltage  $V$  it can at first rise with temperature and only then start to decline.

The dependence of the full critical current on  $V$  is typically highly nonlinear and strongly nonsymmetric with respect to  $V = 0$  due to the interplay of  $j_s$  and  $j_t$ . This also leads to appearance of a number of  $0-\pi$  transitions in the system upon varying controlling voltage  $V$ .



- <sup>1</sup> F.S. Bergeret, A.F. Volkov, and K.B. Efetov, *Phys.Rev.Lett.* **86**, 4096 (2001).
- <sup>2</sup> F.S. Bergeret, A.F. Volkov, and K.B. Efetov, *Rev. Mod. Phys.* **77**, 1321 (2005).
- <sup>3</sup> A.I. Larkin and Yu.N. Ovchinnikov, *Sov. Phys. JETP* **20**, 762 (1965) [*Zh. Eksp. Teor. Fiz.* **47**, 1136 (1964)].
- <sup>4</sup> P. Fulde and R.A. Ferrel, *Phys.Rev.* **135**, A550 (1964).
- <sup>5</sup> A. I. Buzdin, L. N. Bulaevsky, and S. V. Panyukov, *JETP Lett.* **35**, 178 (1982) [*Pis'ma Zh. Eksp. Teor. Fiz.* **35**, 147 (1982)].
- <sup>6</sup> A. I. Buzdin, B. Bujicic, and M. Yu. Kupriyanov, *Sov. Phys. JETP* **74**, 124 (1992) [*Zh. Eksp. Teor. Fiz.* **101**, 231 (1992)].
- <sup>7</sup> V. V. Ryazanov, V. A. Oboznov, A. Yu. Rusanov, A. V. Veretennikov, A. A. Golubov, and J. Aarts, *Phys. Rev. Lett.* **86**, 2427 (2001).
- <sup>8</sup> T. Kontos, M. Aprili, J. Lesueur, F. Genet, B. Stephanidis, R. Boursier, *Phys. Rev. Lett.* **89**, 137007 (2002).
- <sup>9</sup> Y. Blum, A. Tsukernik, M. Karpovski, and A. Palevski, *Phys. Rev. Lett.* **89**, 187004 (2002).
- <sup>10</sup> W. Guichard, M. Aprili, O. Bourgeois, T. Kontos, J. Lesueur, and P. Gandit, *Phys. Rev. Lett.* **90**, 167001 (2003).
- <sup>11</sup> A.S. Sidorenko, V.I. Zdravkov, J. Kehrle, R. Morari, G. Obermeier, S. Gsell, M. Schreck, C. Müller, M.Yu. Kupriyanov, V.V. Ryazanov, S. Horn, L.R. Tagirov, R. Tidecks, *JETP Lett.* **90**, 139 (2009) [*Pis'ma Zh. Eksp. Teor. Fiz.* **90**, 149 (2009)].
- <sup>12</sup> E. A. Demler, G. B. Arnold, M. R. Beasley, *Phys. Rev. B* **55**, 15174 (1997).
- <sup>13</sup> A. A. Golubov, M. Yu. Kupriyanov, and E. Ilchev, *Rev. Mod. Phys.* **76**, 411 (2004).
- <sup>14</sup> A. I. Buzdin, *Rev. Mod. Phys.* **77**, 935 (2005).
- <sup>15</sup> A. F. Volkov and K. B. Efetov, *Phys. Rev. B* **78**, 024519 (2008).
- <sup>16</sup> Ya. V. Fominov, A. F. Volkov, and K. B. Efetov, *Phys. Rev. B* **75**, 104509 (2007).
- <sup>17</sup> Y. Asano, Y. Sawa, Y. Tanaka, and A. A. Golubov, *Phys. Rev. B* **76**, 224525 (2007).
- <sup>18</sup> M. Eschrig, J. Kopu, J. C. Cuevas, and G. Schön, *Phys. Rev. Lett.* **90**, 137003 (2003).
- <sup>19</sup> A.F. Volkov, A. Anishchanka, and K.B. Efetov, *Phys. Rev. B* **73**, 104412 (2006).
- <sup>20</sup> T. Champel, T. Löfwander, and M. Eschrig, *Phys. Rev. Lett.* **100**, 077003 (2008).
- <sup>21</sup> M. Alidoust, J. Linder, G. Rashedi, T. Yokoyama, and A. Sudbo, *Phys. Rev. B* **81**, 014512 (2010).
- <sup>22</sup> M. Houzet and A.I. Buzdin, *Phys. Rev. B* **76**, 060504(R) (2007).
- <sup>23</sup> A.F. Volkov and K.B. Efetov, *Phys. Rev. B* **81**, 144522 (2010).
- <sup>24</sup> R.S. Keizer, S.T.B. Goennenwein, T.M. Klapwijk, G. Miao, G. Xiao, and A. Gupta, *Nature (London)* **439**, 825 (2006).
- <sup>25</sup> T.S. Khaire, M.A. Khasawneh, W.P. Pratt, Jr., and N.O. Birge, *Phys. Rev. Lett.* **104**, 137002 (2010).
- <sup>26</sup> M.S. Anwar, M. Hesselberth, M. Porcu, and J. Aarts, *arXiv:1003.4446* (unpublished).
- <sup>27</sup> I. Sosnin, H. Cho, V.T. Petrashov, and A.F. Volkov, *Phys. Rev. Lett.* **96**, 157002 (2006).
- <sup>28</sup> I.V. Bobkova and A.M. Bobkov, *Phys. Rev. B* **82**, 024515 (2010).
- <sup>29</sup> A.F. Volkov, *Phys. Rev. Lett.* **74**, 4730 (1995).
- <sup>30</sup> F.K. Wilhelm, G. Schön, and A.D. Zaikin, *Phys. Rev. Lett.* **81**, 1682 (1998).
- <sup>31</sup> S.-K. Yip, *Phys. Rev. B* **58**, 5803 (1998).
- <sup>32</sup> T.T. Heikkilä, J. Särkkä, and F.K. Wilhelm, *Phys. Rev. B* **66**, 184513 (2002).
- <sup>33</sup> T.T. Heikkilä, F.K. Wilhelm, and G. Schön, *Europhys. Lett.* **51**, 434 (2000).
- <sup>34</sup> T. Yokoyama, Y. Tanaka, and A.A. Golubov, *Phys. Rev. B* **75**, 134510 (2007).
- <sup>35</sup> Y. Asano, Y. Tanaka, and A.A. Golubov, *Phys. Rev. Lett.* **98**, 107002 (2007).
- <sup>36</sup> V. Braude and Yu.V. Nazarov, *Phys. Rev. Lett.* **98**, 077003 (2007).
- <sup>37</sup> J. Linder, T. Yokoyama, A. Sudbø, and M. Eschrig, *Phys. Rev. Lett.* **102**, 107008 (2009).
- <sup>38</sup> T. Yokoyama and Ya. Tserkovnyak, *Phys. Rev. B* **80**, 104416 (2009).
- <sup>39</sup> J. Linder, A. Sudbø, T. Yokoyama, R. Grein, and M. Eschrig, *Phys. Rev. B* **81**, 214504 (2010).
- <sup>40</sup> K.D. Usadel, *Phys.Rev.Lett.* **25**, 507 (1970).
- <sup>41</sup> M.Yu. Kupriyanov and V.F. Lukichev, *Sov. Phys. JETP* **67**, 1163 (1988).
- <sup>42</sup> Yu.V. Nazarov, *Superlattices Microstruct.* **25**, 1221 (1999).
- <sup>43</sup> D. Huertas-Hernando, Yu.V. Nazarov, and W. Belzig, *Phys. Rev. Lett.* **88**, 047003 (2002).
- <sup>44</sup> A. Cottet, D. Huertas-Hernando, W. Belzig, and Yu.V. Nazarov, *Phys. Rev. B* **80**, 184511 (2009).
- <sup>45</sup> J. W. Serene and D. Rainer, *Phys. Rep.* **101**, 221 (1983).